A STUDY OF DYNAMIC LOADS ON STRAIGHT SPUR GEAR TEETH

PAUL JAY UMBERGER

A STUDY OF DYNAMIC LOADS

ON STRAIGHT SPUR GEAR TEETH

by

Paul Jay Umberger
Lieutenant, United States Navy
B.S., United States Naval Academy, 1961

Submitted in partial fulfillment of the
requirements for the degree of

MASTER OF SCIENCE IN MECHANICAL ENGINEERING

from the

NAVAL POSTGRADUATE SCHOOL
June 1968

ABSTRACT

The dynamic loads acting on gear teeth are very complex. To better understand dynamic loads, this research was carried out with the objectives of measuring experimentally dynamic loads and the frictional forces between gear teeth in mesh. By using strain gages mounted on the sides of the teeth, the transverse component of the dynamic load was measured and is shown for all phases of contact. Using the transverse component at the pitch radius, the dynamic load ratios were computed and found to be substantially lower than predicted by the Buckingham equation. However, sufficient information for evaluating the frictional force was not obtained and further research will be required to evaluate the radial component of the dynamic load.

TABLE OF CONTENTS

LIST OF ILLUSTRATIONS

LIST OF ILLUSTRATIONS (CONT'D)

ACKNOWLEDGEMENTS

The author wishes to extend his sincere appreciation to Professor E. K. Gatcombe for his patience and guidance during the course of this investigation. Many thanks are also due to Mr. M. J. O'Dea of the Machine Facility of the Naval Postgraduate School for the care and skill shown in the fabrication of the single-tooth calibration device.

1. Introduction.

The interacting forces between two teeth when gears mate are very complicated and poorly understood. On the other hand, the conjugate action of gears is well understood. It has been learned through experience and testing that the dynamic load depends upon the velocity of the rotating teeth and the accuracy of the tooth profile as the gear was manufactured. Each particular physical application for which the gear is used has different characteristics.

This experimental research is undertaken for the purpose of learning more about actual dynamic loads. The investigation has two primary objectives: Firstly, to establish that dynamic loads on gear teeth can be measured. Secondly, to show that the resultants force on the gear tooth may be determined by measuring the radial force on the tooth as well as the transverse component of the dynamic load. Knowing the resultant force on the tooth, the frictional component of that force can be computed.

This investigation was carried out in the following phases: instrumentation of the gear, calibration of the instrumentation, dynamic testing, and analysis. The purpose of the extensive calibration is to interpret the experimental data in units of force.

2. General Discussion.

The load carried by gear teeth is said to be composed of the load transmitted through the gear train plus the additional load caused by the dynamic effects of the mating pair of teeth. It has been found that this total load can often be several times as great as the transmitted load.

The dynamic component of the load on gear teeth is brought about by the impacting masses of the gears and the connected components, as they accelerate and decelerate, and by the torsional elasticity of the shafts. The accelerations are produced by irregularities in the tooth profile called tooth errors. As the teeth engage and pass through contact, tooth errors cause one gear to change speed. The two contacting surfaces attempt to separate, but the driving power and the gear train load act to resist this separation. The re-engagement that follows produces an impact load on the teeth.

Tooth error results primarily from the inherent manufacturing inaccuracies. The most important parts of tooth error are profile error, indexing error, and radial runout. Although these errors can be controlled by regulating manufacturing processes, they cannot be eliminated. They can, however, be measured after the gear has been made.

Extensive work has been done by Professor Earl Buckingham on the dynamic loading of gears. He states that the dynamic action of the gear teeth results in pressure pulses on the teeth. One pulse occurs when the pair of teeth engages and picks up the load. Another pulse occurs at the time of impact of the teeth after separation [1]. He further suggests that the magnitude of the force required to keep the surfaces from separating is dependent upon the magnitude of the tooth error rather

than the nature of that error.

As a result of his work, the equation of dynamic loads on spur-gear teeth developed by Buckingham [1] is

$$Fd = Ft + \sqrt{f_a(2f_2 - f_a)} \quad \text{where}$$

Fd = dynamic load, lb.

Ft = transmitted load, lb.

f_a = acceleration load, lb.

f_2 = limiting acceleration load, lb.

It is felt that Buckingham's equation is too conservative for applications where low power is transmitted. Since the power transmitted in my test unit is less than six horsepower, an empirical equation recommended by the AGMA will also be used for comparison [2].

$$Fd = \left(\frac{50 + v_m}{50} \right)^{\frac{1}{2}} Ft$$

is for commercially hobbed or shaved teeth where v_m is the pitch line speed in feet per minute. The service factors and load distribution factor normally used in gear design will not be added in this comparison.

An experimental study of dynamic loading of gear teeth was made by John A. Pethick, II [4]. His method used in evaluating the dynamic load was one of relative magnitude ratios. Output pulses from a strain gage bridge were evaluated at the pitch point phase only. No information can be obtained from his work as to the distribution of force on the tooth as it passes through the other phases of contact. The pitch point phase might or might not be where the maximum dynamic load occurs.

For this investigation the gears and the four-square gear testing device used by Pethick was used, but the instrumentation is completely different, as well as the methods of evaluation.

3. Gear Instrumentation.

In order to evaluate the resultant force on the gear tooth, two components of that force need to be known. The first component measured was that force whose direction is parallel to the tangent to the pitch circle, called the "tangential force", Ft. The torque is equal to the product of the tangential force at the pitch radius and the radius. It can be seen that if only one pair of teeth are in contact and there are no dynamic effects, the transmitted force and the tangential force can easily be related.

The second component measured is in a radial direction and will be referred to as the "radial force", Fr.

Measuring the strain at a point on the tooth and then calculating the stress and the forces is impractical. The stresses in the tooth are complex. The tooth is small and a very small strain gage would be needed to measure a simulated point strain. Therefore, strain gages were installed and calibrated to provide signals directly related to the force.

From figure 1, it can be seen that the resultant force on the tooth, $\overline{F}$, is the vector sum of $\overline{Ft}$ and $\overline{Fr}$. The same total force, $\overline{F}$, is also the vector sum of the force, $\overline{N}$, acting normal to the profile at the point of contact, and the friction force, $\overline{R}$, acting along the profile surface. Hence if the total force, $\overline{F}$, is known by measuring $\overline{Ft}$ and $\overline{Fr}$, it is a simple matter to find the magnitudes of $\overline{N}$ and $\overline{R}$, since their directions are known for any contact point.

The most severe stress condition in the gear tooth would exist when the load is applied at the tip of the tooth. Neglecting friction, the load is applied normal to the tooth profile. If the tooth is approximated by a beam of uniform strength, or a parabolic beam whose vertex is at the

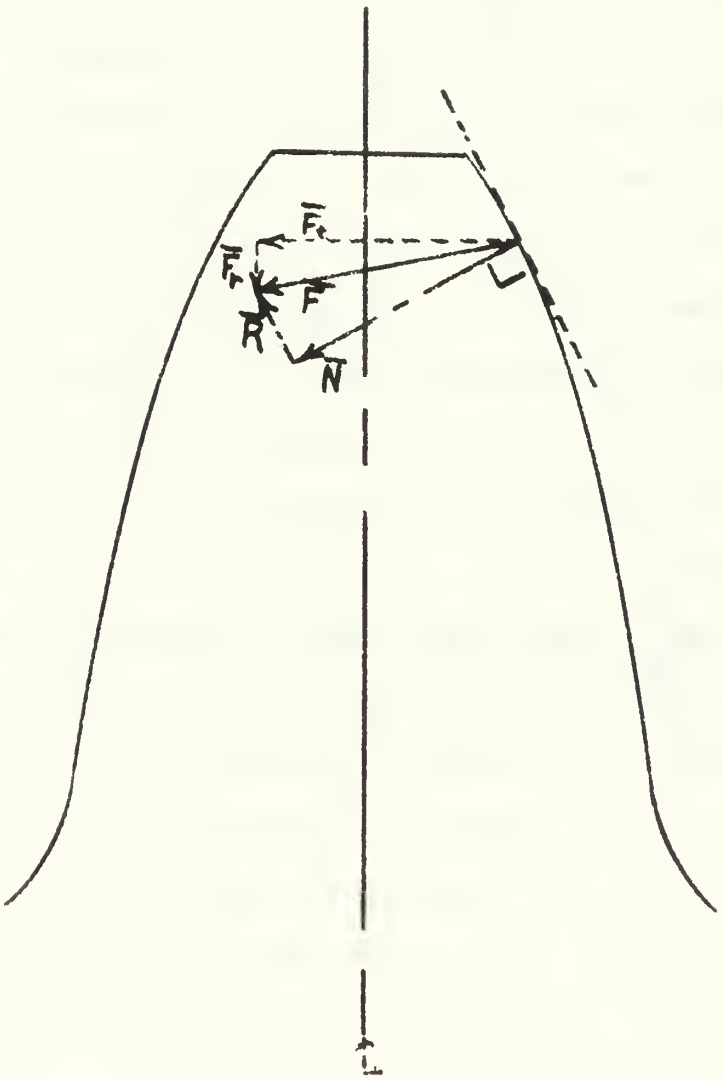

Figure 1. Components of Force Acting on a Gear Tooth

point where the frictionless load direction intersects the tooth center line, the section of maximum stress will be located at the section where the inscribed parabolic beam is tangent to the involute profile. This section of maximum stress, noted as section A-A on figure 2, is the best location for strain gages.

To locate this section on the particular tooth, the actual tooth profile was expanded fifty times by using a shadowgraph. Using the shadowgraph trace, the inscribed parabola was graphically constructed using a method outlined by H. D. Merritt [3]. The section of maximum stress was found to be 0.173 inches from the tip of the tooth.

A plastic template was then made to use in placing the strain gages on the teeth. A sharp scribe was used to imprint the tooth profile and the profiles of several adjacent teeth on the plastic. The tooth center line and the position of the maximum stress section were also inscribed on the template.

A single-element strain gage was cemented onto one side of the gear tooth to measure the strain caused by radial forces. Figure 3 shows the gage locations on the tooth. The radial force gage was placed on the center line of the tooth, which is the neutral axis of the tooth. With this orientation, the gage will be sensitive only to forces in the y-direction, Fy, and moments about the x-axis, Mx. Moments about the x-axis do not exist in this application. Fr is directed identically with Fy and the gage will pick up only radial strains.

To measure the tangential force acting on the tooth, a two-element ninety-degree strain gage rosette was cemented onto the other side of the tooth. This rosette measures the shear strain at the section of maximum stress. Each gage element is oriented 45 degrees on either side of the

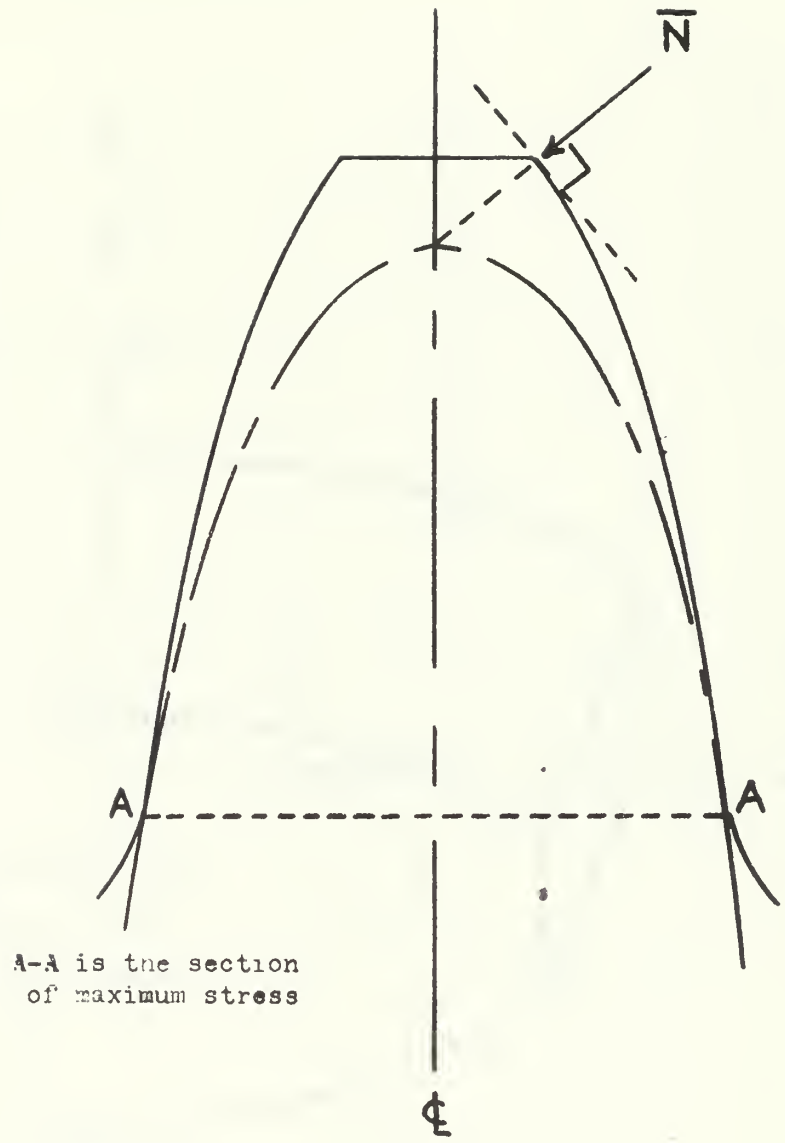

Figure 2. Section of Maximum Stress

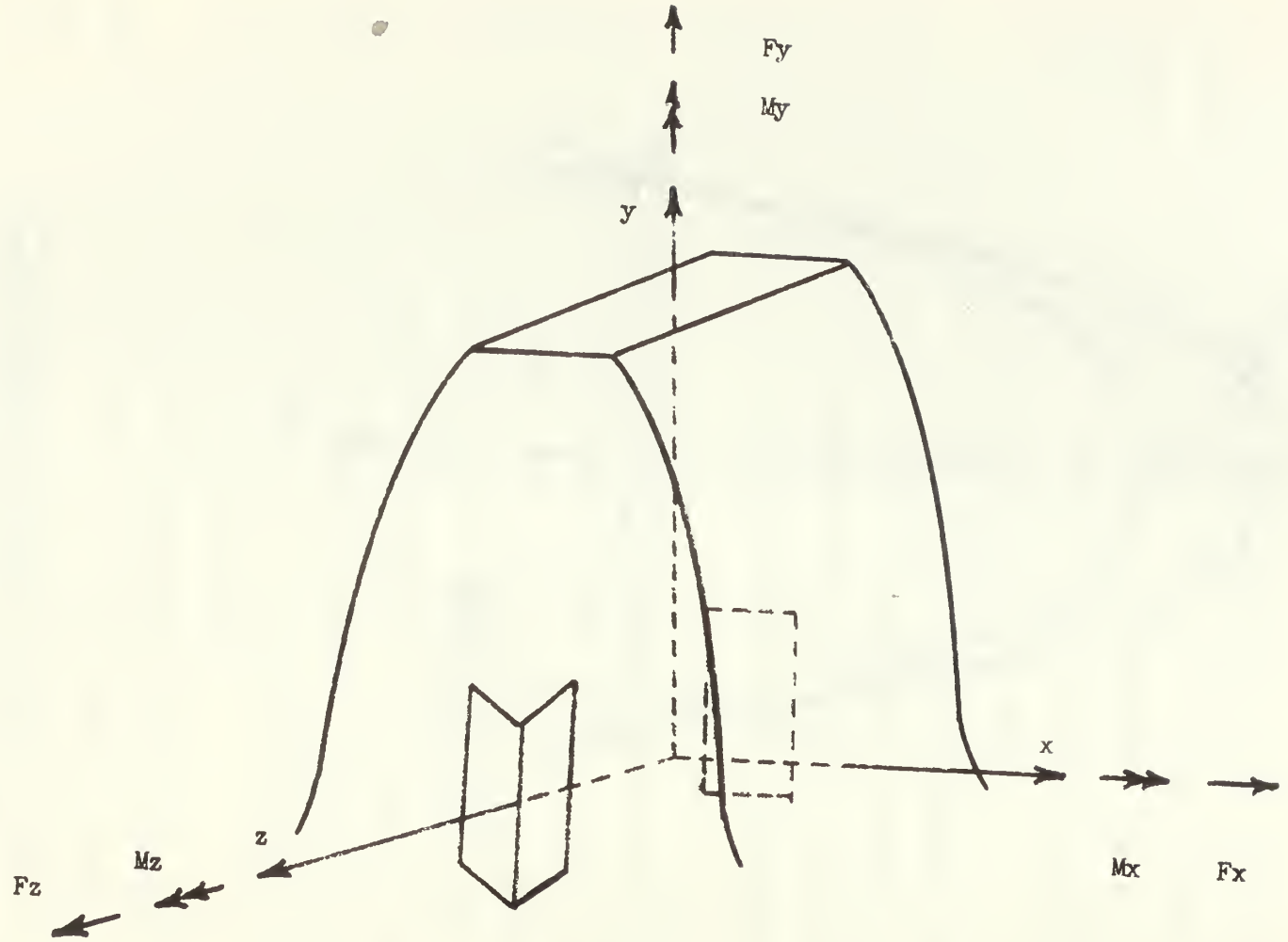

Figure 3. Gear Tooth Coordinate System

tooth center line as shown in figure 3. Using two dummy gages to complete the four arm Wheatstone bridge, the following matrix representation shows what forces will affect the bridge.

$$\begin{matrix} & & 1 & 2 & 3 & 4 & & B_1 & B_2 & B_3 \\ \begin{bmatrix} Fx \\ Fy \\ Fz \\ Mx \\ My \\ Mz \end{bmatrix} & = & \begin{bmatrix} 1 & -1 & 0 & 0 \\ \frac{1-\mu}{2} & \frac{1-\mu}{2} & 0 & 0 \\ 0 & 0 & 0 & 0 \\ -\left(\frac{1-\mu}{2}\right) & -\left(\frac{1-\mu}{2}\right) & 0 & 0 \\ 1 & -1 & 0 & 0 \\ 0 & 0 & 0 & 0 \end{bmatrix} & & \begin{bmatrix} -1 & -1 & -1 \\ 1 & 1 & -1 \\ -1 & 1 & 1 \\ 1 & -1 & 1 \end{bmatrix} \end{matrix}$$

$$\begin{matrix} & & B_1 & B_2 & B_3 \\ \begin{bmatrix} Fx \\ Fy \\ Fz \\ Mx \\ My \\ Mz \end{bmatrix} & = & \begin{bmatrix} -2 & -2 & 0 \\ 0 & 0 & -(1-\mu) \\ 0 & 0 & 0 \\ 0 & 0 & (1-\mu) \\ -2 & -2 & 0 \\ 0 & 0 & 0 \end{bmatrix} \end{matrix}$$

where 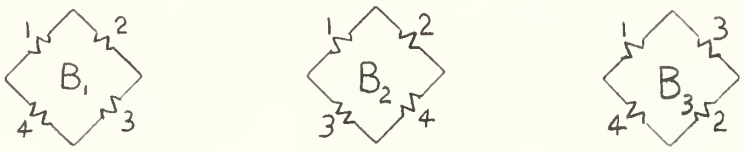

and gages 1 and 2 are always active with 3 and 4 inactive.

From this matrix symbolization it can be seen that with either B_1 or B_2 the bridge will be sensitive only to Fx and My. Both bridges will

have a bridge factor of (-2). For simplicity reasons the 1-2-3-4 hook-up of bridge B_1 was chosen.

The particular gears in use have been used in previous studies [4] and have been well run-in. The gears are of good quality and contact across the tooth face can be considered to be uniform. With uniform contact there will be no moments applied to the instrumented tooth about the y-axis. The only force to which the gage rosette is sensitive is Fx, which in this case is directed identically with tangential force, Ft.

Foil strain gages with epoxy backing were used. EPY 400 cement was used to secure the gages to the gear. Further characteristics of the gages, cement, and wire can be found in Appendix B.

Temperature compensation of the gages is required, and because different lengths of wire in the bridge connections affect the bridge output, the four gage Wheatstone bridge was completed right on the instrumented gear. Locating these compensating gages on the web of the gear is not satisfactory because the web strains, small though they may be, will be picked up by the gages. For this reason all of the compensating gages were located on other teeth as shown in Figure 4. No two of the four teeth mate simultaneously and the compensating gages are in a strain-free condition.

The gages were carefully arranged using the plastic template and cemented to the gear. Note that two of the teeth are identically instrumented. Each has a two-element rosette on one side and a single gage on the other side. The other two gages used to complete the radial strain bridge were located on randomly chosen teeth. This random spacing will later assist in identifying the pulses from the two instrumented teeth.

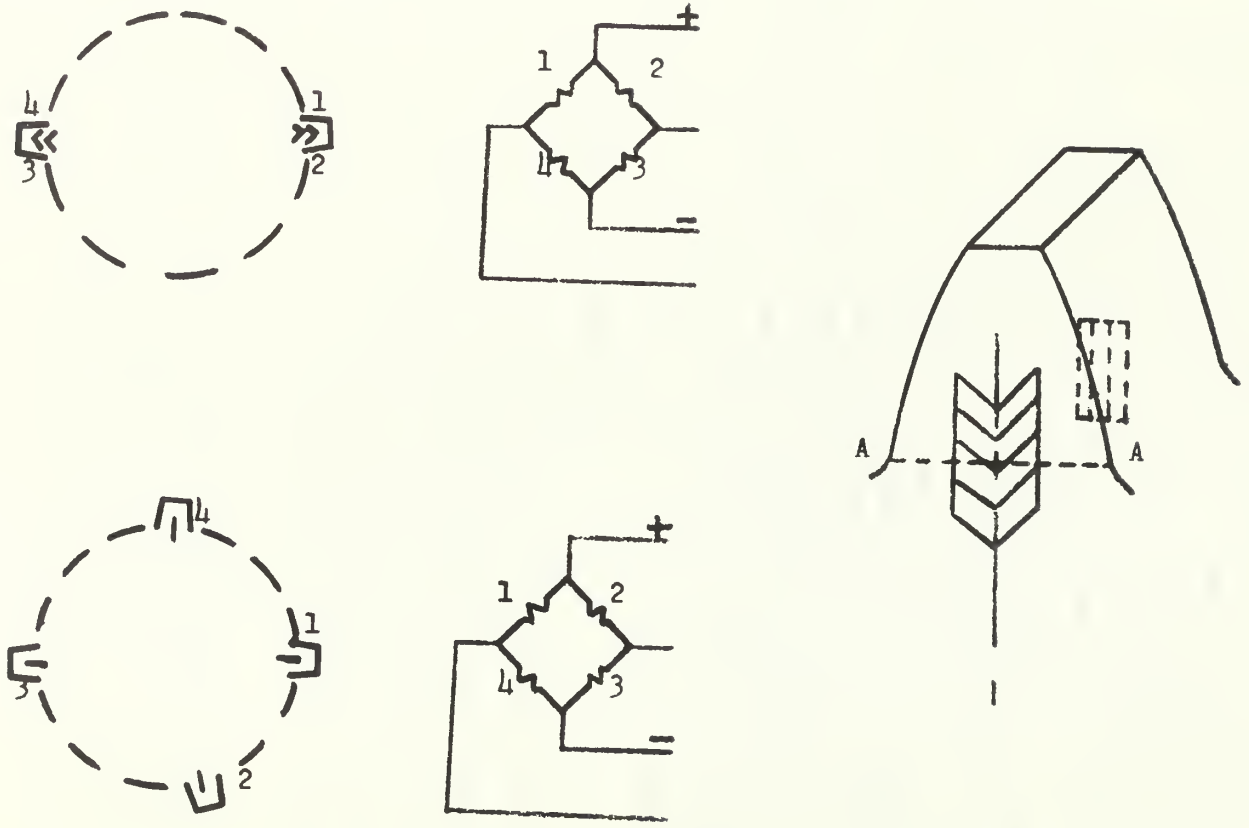

Figure 4. Location of Strain Gages on the Gear

The four-square gear testing maching was designed by H. J. Hansen, III [5]. It was assembled and first used by J. A. Pethick, II [4]. The construction and operation of the machine is covered in detail by their works. Basically, the four-square gear test rig consists of two parallel shafts with test spur gears in mesh at one end of the shafts. Helical gears are splined onto the shafts near the other end. One of the helical gears is moved in the axial direction by means of a hydraulic piston. When the helical gear is moved axially, it twists the shaft, thereby loading the test gears. A six horsepower DC motor coupled to one shaft rotates the gears.

To measure the force transmitted through the gears, a torsion bridge is installed on the shaft of the instrumented gear. The torsion bridge installed by Pethick was carefully checked and calibrated by me but was not changed.

4. Calibration.

The first step in the calibration procedure was to calibrate the torsional strain bridge. The bridge is located on the shaft connecting the instrumented gear and one of the helical gears of the four-square gear test device. Access to the bridge was not required nor was it possible since the section of the shaft on which the bridge was installed is within the drive section of the four-square device.

For calibration, the shaft was prevented from rotating by connecting a brass strap from the flywheel on one end of the shaft to the foundation base plate. With both test gears removed, a bracket was pinned to the other end of the shaft. One end of a 28-inch arm was then bolted to the bracket in such a way that the arm was free from interference of the second shaft of the test machine. This arm was notched at measured intervals to accommodate a weight pan.

A Baldwin-Lima-Hamilton type "N" strain indicator was used to measure the torsional bridge strain. The strain was measured for various known moments. Measured weights were added at a moment arm of twenty inches to produce moments up to 457 inch-pounds including the moments of the arm and the pan.

The torsion computed from the strain gage measurements was plotted vs. the torsion as obtained from leverage. In all cases, the leverage torsion was less than the strain gage torsion for a specified strain as shown in figure 5.

This procedure was repeated for three random angular positions of the shaft. In all cases the results were so close as to indicate no difference.

Before proceeding with the calibrations of the strain gage bridges on the gear, it would be good to note what might be expected. If we

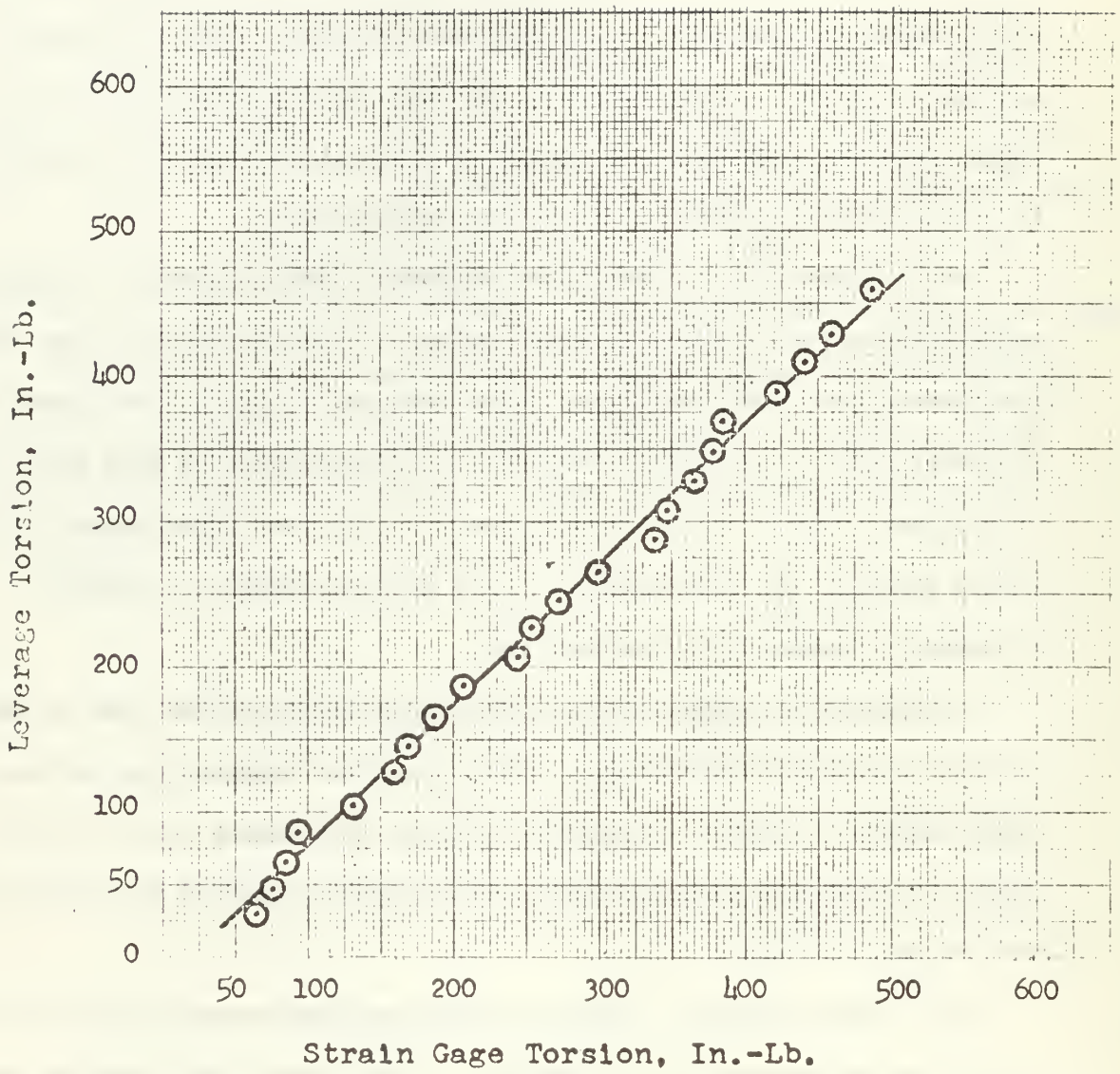

Figure 5. Torsion Bridge Calibration

consider the tooth to be a basic cantilever beam, we would expect that the shear bridge reading should not change for a specified force in the tangential direction no matter where the force is applied, as long as it is not applied too close to the gage section. Likewise, we would expect the strain to increase uniformly as the force increases.

We would expect the radial strain on the neutral axis to be independent of the angle of application of the resultant force as long as the radial component of that force is the same. Again we would expect the radial strain to increase linearly as the radial force increases.

We must bear in mind, however, that the gear tooth is not in fact a uniform cantilever beam. Also the relative size of the strain gages and the tooth might lead us to expect some variation. Difficulties in installing gages exactly on the neutral axis of the tooth and at the maximum stress section might also cause errors and the results should only approximate beam theory at best.

Calibration of the gear strain gage bridges was accomplished in two phases. The first phase involved the application of varying forces at the same point on the tooth. This was done by loading the tooth with weights suspended from a wire. This first phase will be referred to as the "wire calibration".

A 0.025-inch diameter hole was drilled through the tooth at a distance of 0.050 inches from the tip of the tooth on the tooth center line before the strain gages were cemented to the gear. A slight error resulted in drilling this small hole through the hardened material. Drilling was started properly but the drill emerged slightly off center on the other side of the tooth. This should be kept in mind but a large error should not result.

A stainless steel wire with a diameter of 0.024 inches and a test strength of about 119 pounds was run through the hole. The ends of the wire were spliced together to make a loop. A small ball bearing with a groove in which the wire could ride on the outside of the bearing outer race was fitted over the gooseneck of a weight pan. The purpose of the bearing was to insure equal tension in each side of the wire loop.

With the gear hub firmly clamped in a bench vise, weights in the range of 0 to 90 pounds were suspended from the wire on a weight pan as shown in figure 6, while the radial and shear bridge reading were taken. Baldwin-Lima-Hamilton type "N" strain indicators were used to measure the strain.

After suspending the weights, the gear was slightly rotated in the vise. Weights were suspended and readings were taken for all possible angles. Certain angles of suspension were prohibited by the interference of the vise and the bench. In one case, the force was directed radially inward toward the center of the gear by using a spanner bar through the hole in the gear hub. The spanner bar kept the wires away from interference in this case.

Knowing the angle at which the wire was suspended, the radial and tangential components of the force were computed. These force component values were then plotted versus strain. The plot of tangential force versus strain in figure 7 shows a definite linear relationship. The shear strain is independent of the angle of application of the force. It is also evident that there is a slight change in slope of the line in the two quadrants. This is undoubtedly due to a slight misalignment of the strain gage rosette. It may not be exactly on the tooth center line. For one run, there was slight slippage of the gear hub in the vise and

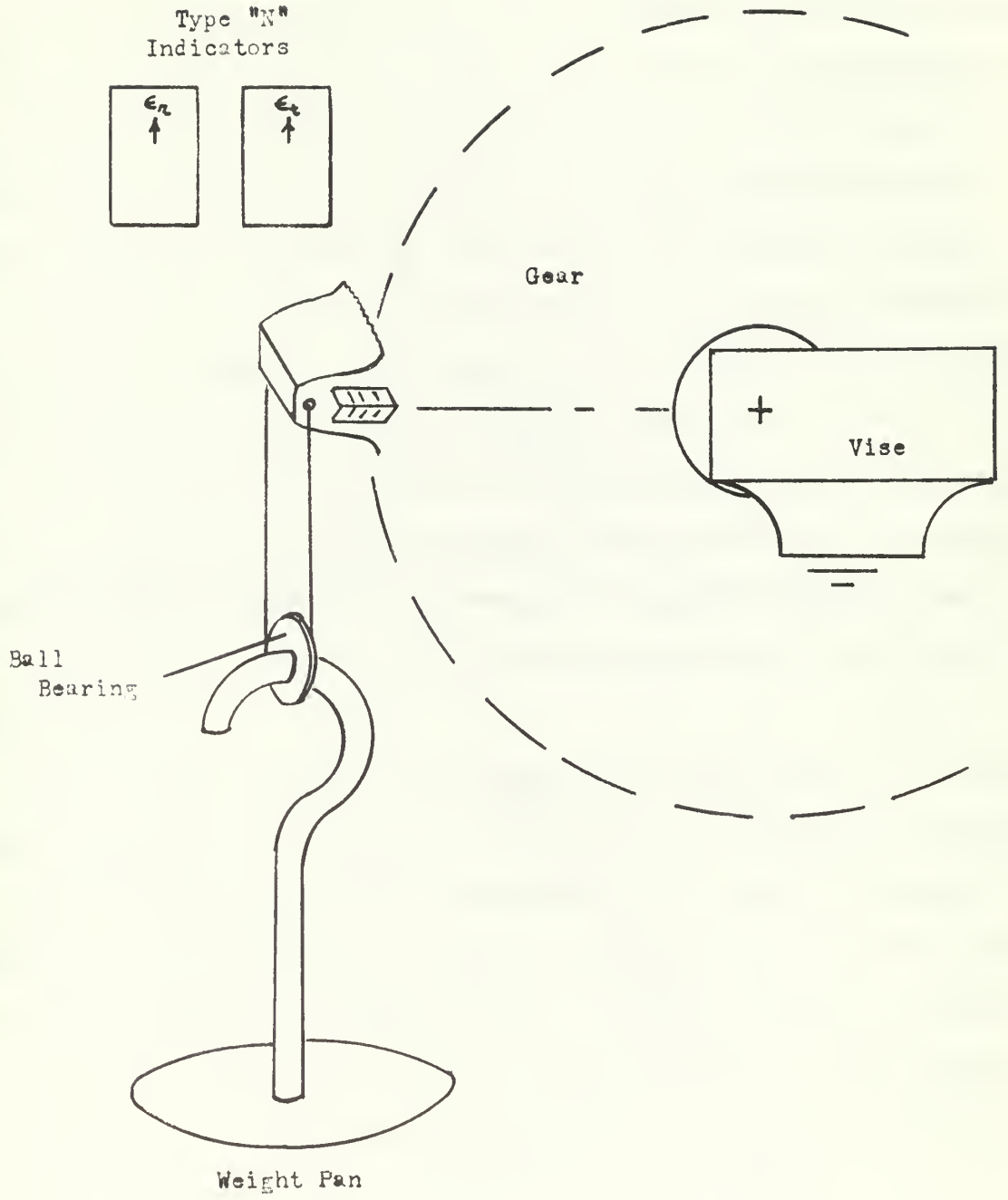

Figure 6. Wire Calibration Apparatus

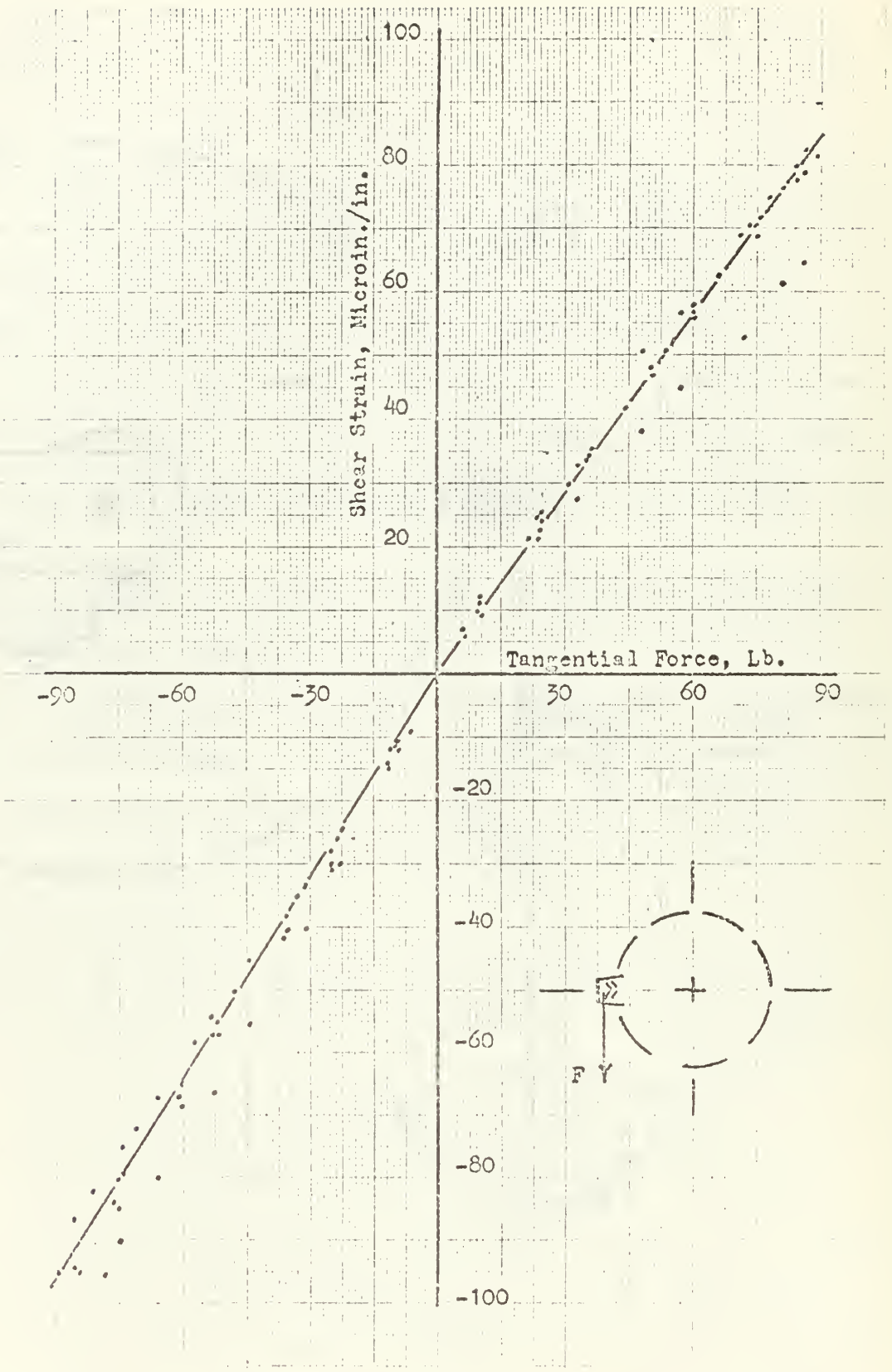

Figure 7. Wire Calibration for Tangential Force

the angle of suspension changed, unnoticed until the end of the run.

The plot of radial force versus strain is shown in figure 8. Again we notice the change of slope due to gage misalignment. There are fewer data points on the positive force side of the plot than on the negative side because of the difficulty in directing the force inward toward the center of the gear. Serious damage to the delicate gage connections could result from suspending the wires directly over the strain gages.

The quadrant in which the data points fall is, of course, dependent upon the strain indicator connections and the definition of positive force. The direction of positive force is defined on each plot.

The purpose of the second phase of the calibration was to apply forces to the instrumented tooth at known points along the profile. An involute mating surface was designed for this purpose. Since the surfaces were well lubricated, conditions closely simulating actual gear tooth action were created.

The gear with which the instrumented gear normally mates in the four-square device could not be used for calibration. A contact ratio greater than one prohibits applying the transmitted force to only one pair of mating teeth for all phases of contact. The contact ratio for this particular set of gears is 1.84 and therefore, one tooth may carry the entire load for only a small fraction of the total contact path. What portion of the transmitted load is carried by only one pair of teeth is unknown and is an integral part of the objectives of this thesis.

The single-tooth gear was designed by me and manufactured by the Machine Facility, Public Works Department of the Naval Postgraduate School. From the drawing reproduced in figure 9, it can be seen that the hub can be pinned to the shaft of the testing device. The single-tooth gear is then bolted securely onto the hub. The curved slots in the hub and the

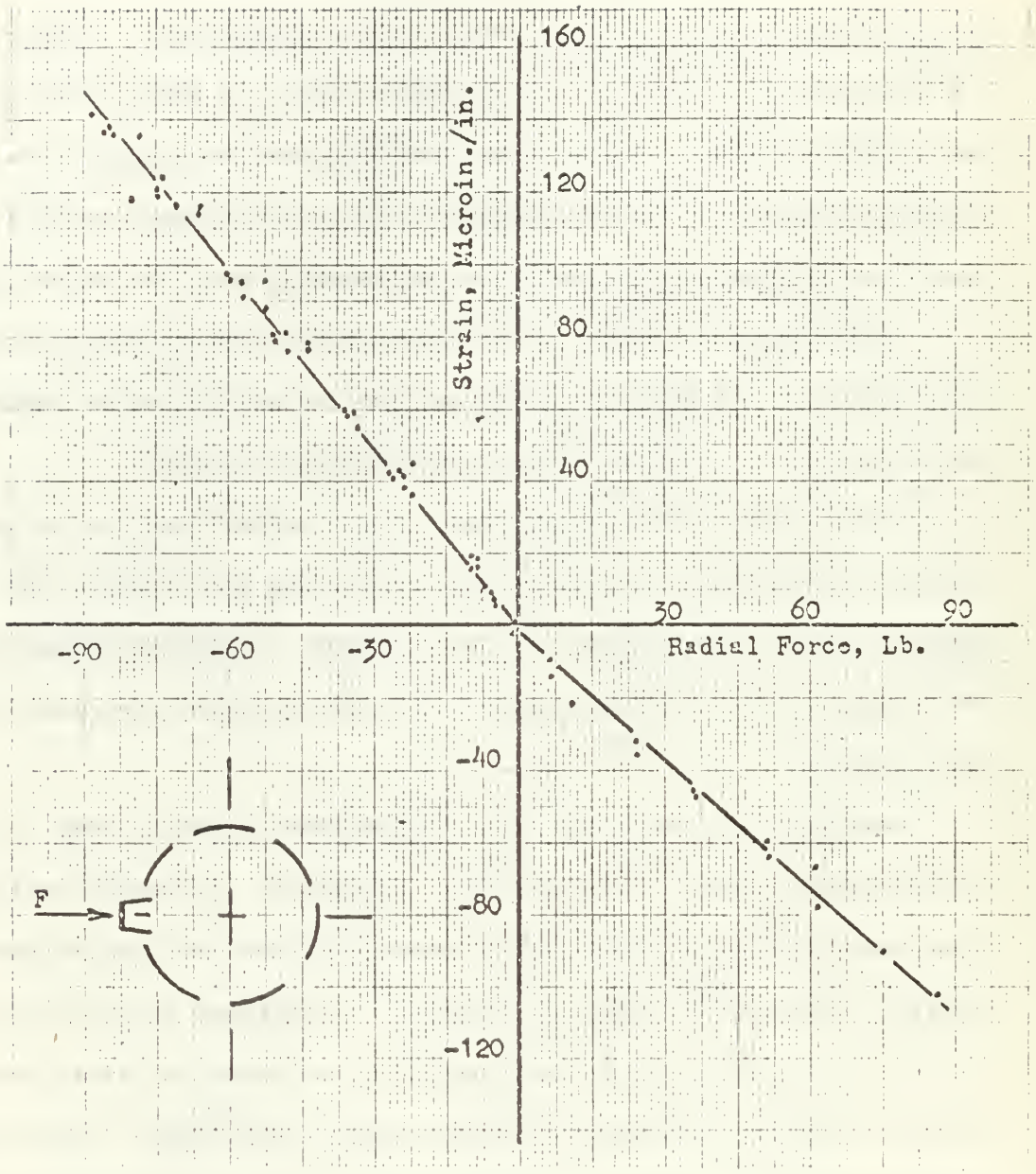

Figure 8. Wire Calibration for Radial Force

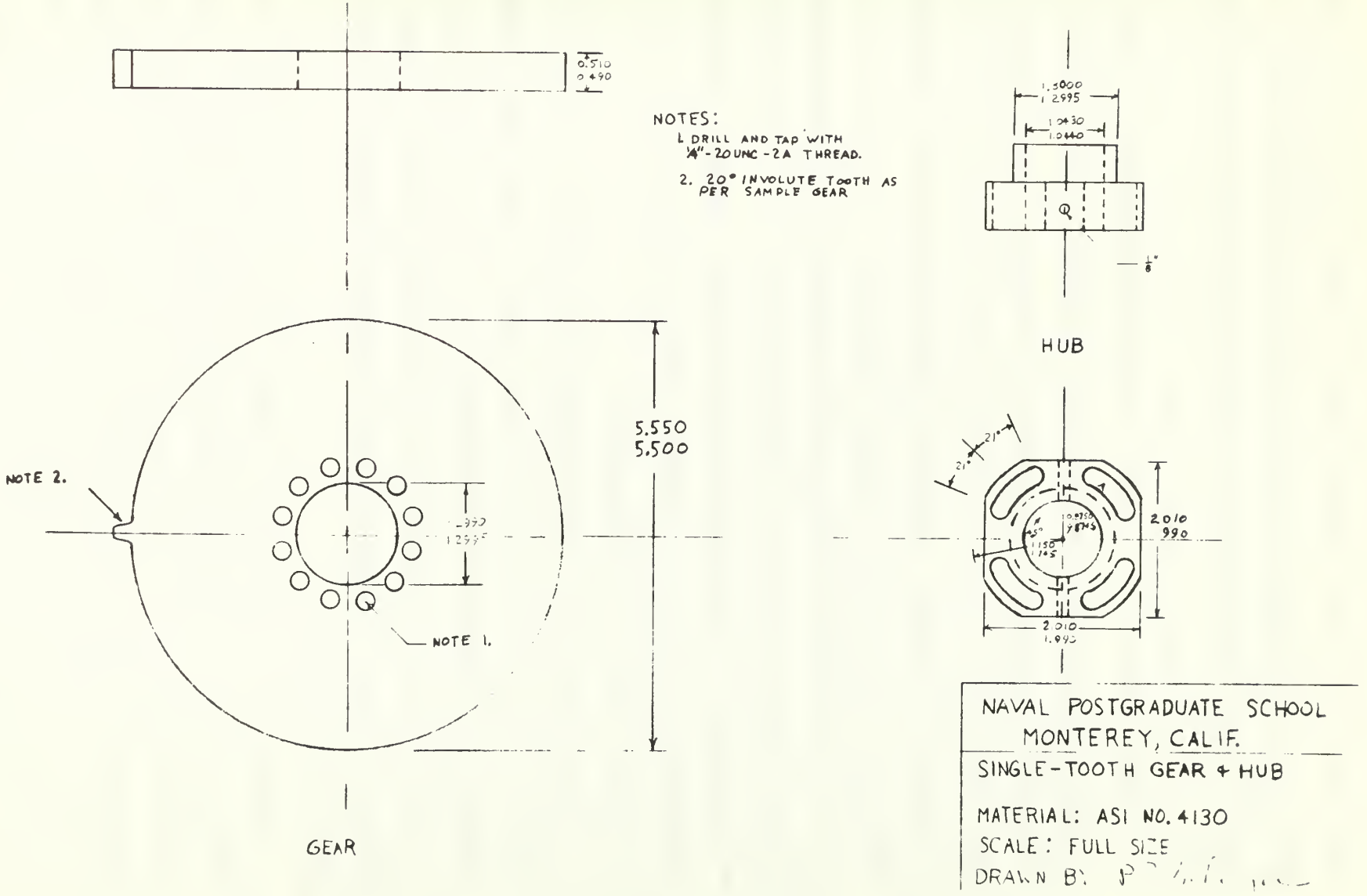

Figure 9. Single Tooth Gear and Hub

holes in the gear permit complete freedom in positioning the tooth. Any tooth on the instrumented gear can be mated with the single tooth while the hub of the single-tooth gear is pinned to the shaft in the same position.

During machining, the clearance between the single-tooth gear and the hub was held to a minimum. It may be recalled that the shear gages are sensitive to moments about a radial line through the gear center. If there is any excess clearance between the single-tooth gear and the hub, or the hub and the shaft, non-uniform tooth face contact will cause such a moment and the calibration will be meaningless.

After the single-tooth gear had been manufactured, it was installed and mated with the test tooth. Blueing was applied to the single tooth and the teeth were manually passed through contact. The high spots on the single tooth face were repeatedly stoned until uniform face contact was achieved through all mating phases.

For this calibration, four parameters were measured. The torsion was measured using a BLH type "N" strain gage indicator. The point of contact between the two teeth was found by measuring the distance from the tip of the instrumented tooth to the point of contact using a Bausch and Lomb graduated microscope. Shear and radial strains were measured with BLH type "N" strain indicators.

With no load on the gears, the single tooth gear was positioned and bolted to its hub. The strain meter zero readings were recorded. A small load was then applied and held while strain readings were recorded. The distance to the contact point was measured using the tip of the instrumented tooth as a reference. The load was then increased and the strain readings were repeated. At each load the distance to the contact point was checked but not recorded because with no rotation, the point of contact

remained the same.

After maximum load had been attained, the gears were unloaded. The meter zero readings were then checked and the point of contact was changed by slightly turning the gear. This process was repeated for many points of contact along the tooth face.

During this calibration it was noted that there was some carry-over between bridge circuits. With all three circuits energized, meter fluctuation occurred on all strain instruments. With any one of the circuits de-energized the fluctuations stopped. Shielded cables were used between the patch board and the instruments. However, the wire leads through the hollow shaft and slip rings to the patch board were not shielded. Ground checks and checks between the circuits were made but no grounds were found. The slip rings were checked and cleaned but there was no improvement.

It was also noted very early in the calibration procedure that little or no useful information was being obtained from the radial bridge. Under static conditions with the surfaces well lubricated, the radial force was expected to be small. It was, in fact, too small. At no time was the reading over five or six microinches per inch. Since these readings were of no use, the radial strain bridge was de-energized and the calibration continued without the bothersome meter fluctuations. Radial readings were rechecked frequently at other contact points but the data remained useless.

The tangential force on the instrumented tooth was calculated using the torsion, as corrected by the torsion calibration, and the radius to the point of contact. This tangential force was then plotted versus the shear strain on a large graph. Figure 10 is a reproduction of this graph.

The data from this calibration plotted very nicely for experimental work. The points for each run, or for each radius, plotted very close to

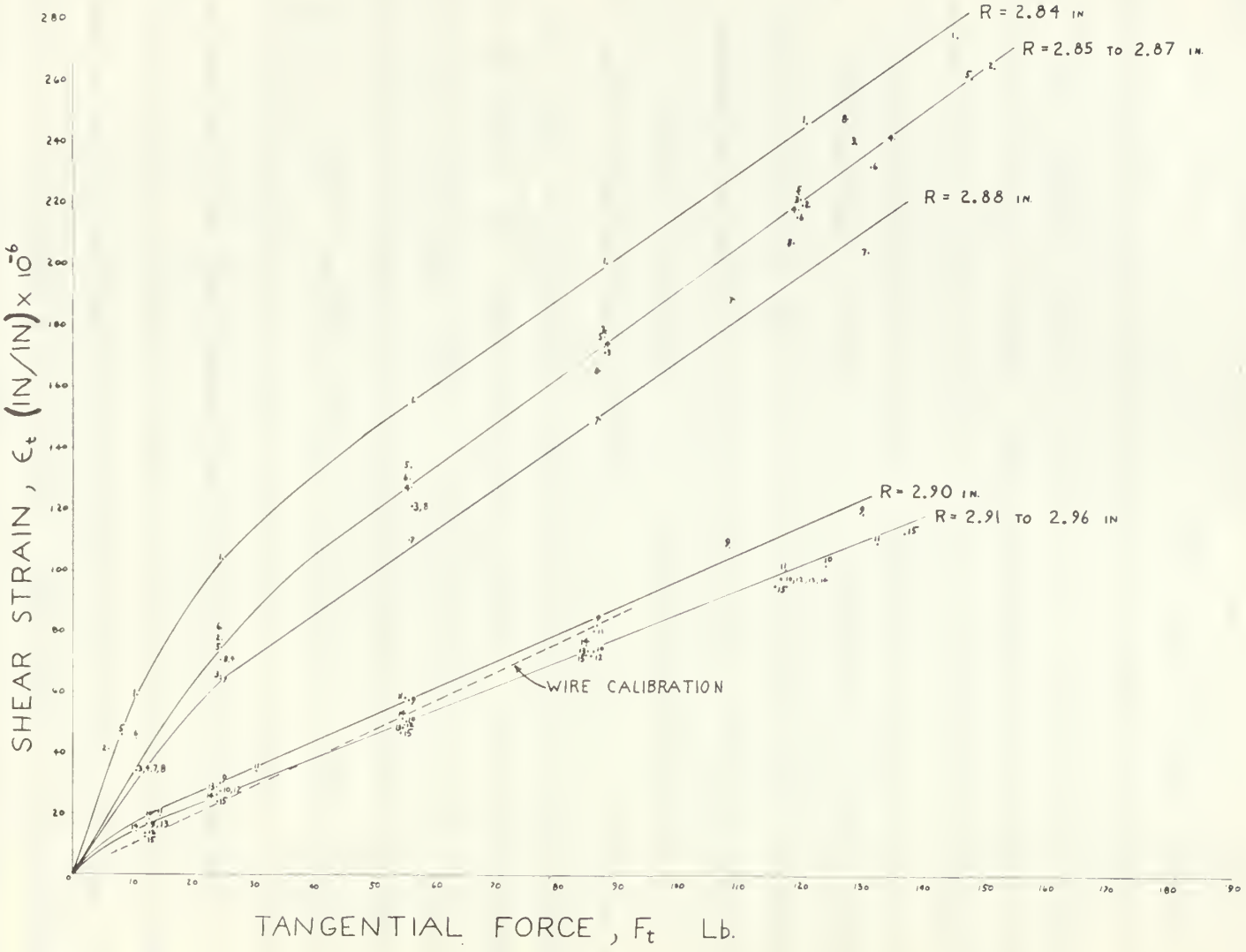

Figure 10. Single-Tooth Gear Calibration Results

a continuous curve. There was considerable "bunching" of the data points but not without reason.

It can be noticed that some of the closely grouped data is slightly out of order. For example, the points for run number 5 are above those for run number 4 instead of below as they should be. The radii data were collected and calculated to four-decimal accuracy. However, when considering the accuracy to which the exact point of contact of the two tangent involute curves could be seen through the oil film, this slight error in order was quite acceptable. The magnitude of the incorrect order of the data points was well within the error limits of the contact point reading.

Since the data points plotted so closely for several radii, a single curve was drawn and the radius range was noted on the plot. It will be recalled from earlier discussion that if the tooth is acting like a cantilever beam, the strain readings for different radii should be the same. This is what caused the bunching.

The dotted line on the graph indicates the results of the wire calibration. As can be seen, the wire calibration falls in the proper place. Considering the vastly different methods, the results of the two calibrations correlate very well.

Since the data as plotted in figure 10 is neither useful as a calibration curve, nor very revealing as to what happened, it will be used merely as a means to an end.

To obtain a useful set of curves, values of the radius and the corresponding tangential force for a constant strain were extracted from figure 10. Curves of constant strain were then plotted on a graph of tangential force versus radial distance to the point of contact. This final and useful plot can be seen in figure 11 and will hereafter be referred to as the "calibration curves".

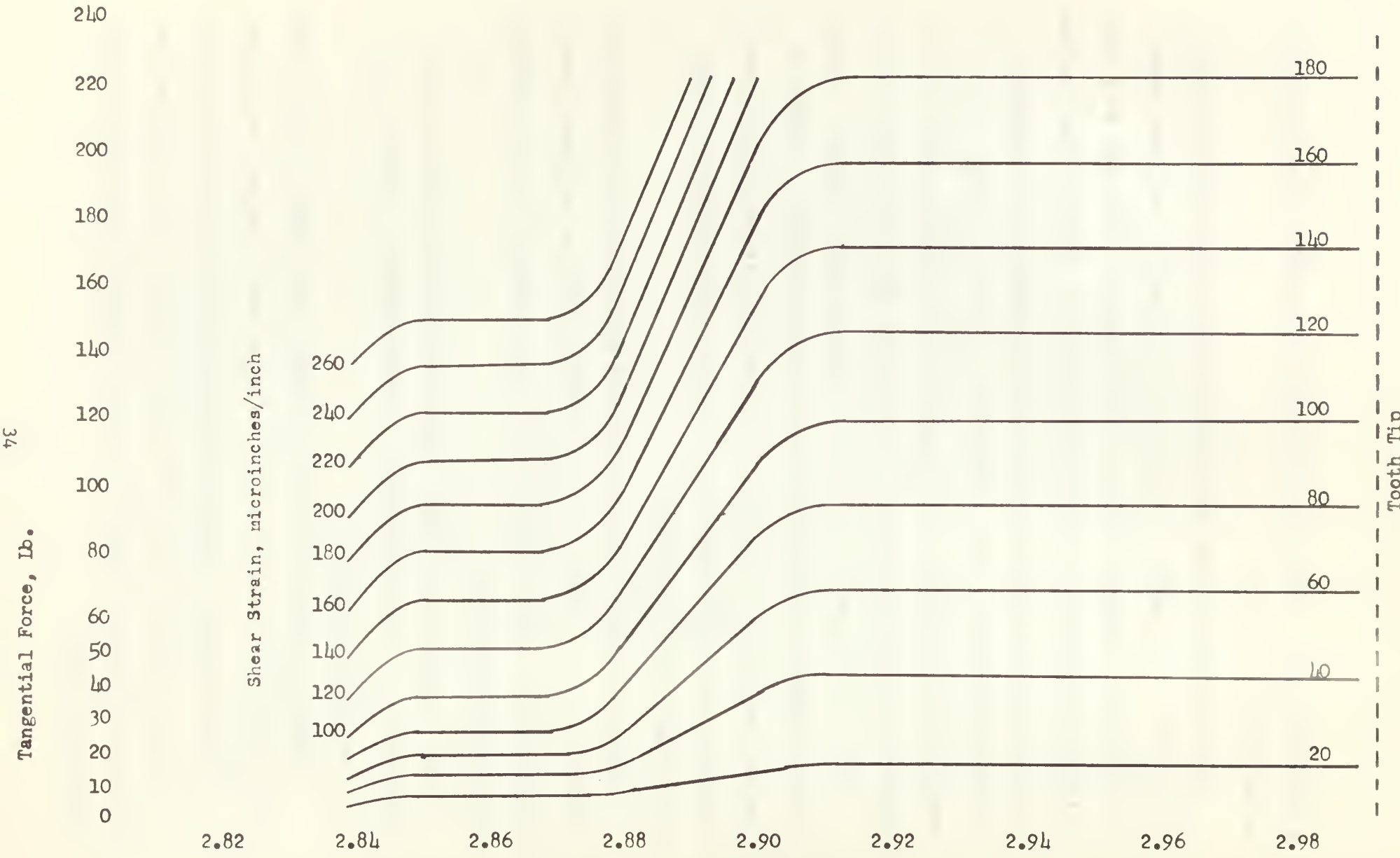

Figure 11. Calibration Curves

Several sections of the calibration curve bear explanation. For example, the right portion of the calibration curve indicates that the tooth is acting as a simple cantilever beam. For an equal tangential force applied between a radius of 2.91 inches and the tip of the tooth, the shear strain bridge output does not change. Also in this region the shear strain increases in direct proportion to the force.

The overall length of the strain rosette was 0.14 inches. With the center line of this gage located 0.173 inches from the tooth tip, the outer end of the gage would be approximately 2.89 inches from the center of the gear. As the applied force moves inward from a radius of 2.91 inches, it approaches and passes the section at the tip of the strain gage. The portion of the calibration curve between 2.91 and 2.87 inches indicates that in this region the strain changes very rapidly with radius. This should be expected.

Between the radii of 2.87 and 2.85 inches another portion of the curve is independent of the radius. At this position the force is at the sections passing through the gages. The reason for the flat section is unexplained. One of the gages of the rosette is normally in compression and the other gage is in tension. These effects are normally additive to produce the bridge factor of two. For some reason the two strains are counteracting each other to produce the linear effect.

At low radii the curves appear to dive. Although this is also unexplained, it is possible that either the contact stresses or the stresses in the gear web are affecting the strain gages. Since the force is now well over the gage, dead spots in the outer end of the gage could also affect the strain gage bridge output.

5. Dynamic Testing.

For the dynamic investigation, the shear and radial bridges were connected to balancing and calibrating amplifiers. Ellis Associates Bridge and Amplifier units were used.

As shown in figure 12, the outputs from both bridges were fed into a dual beam oscilloscope. Both traces were displayed on the scope at the same time. The oscilloscope was triggered by a sine wave from a low frequency function generator. This permitted triggering the scope in synchronization with the rotation of the gears. The trace could then be stabilized on the oscilloscope screen.

When the testing machine was in operation, the speed of rotation varied slightly. The frequency of the function generator had to be adjusted continually to keep the traces on the screen. A scaler timer-counter was used to measure the frequency of the function generator over a period of one hundred seconds while the oscilloscope trace was kept centered on the screen. This provided an accurate measurement of the speed of rotation in units of revolutions per second.

A memory unit in the form of a storage oscilloscope was added in which the scope traces were stored for photographing. This oscilloscope had a single channel capability. Photographs could not be taken from the dual beam scope because the pulses could not be stabilized.

With the test rig in operation, the signal chopping circuit in the BA-2 was engaged for balancing the bridge. While observing the oscilloscope trace, the balancing resistor knob on the BA-2 was adjusted until all evidence of the chopping had disappeared. The magnitude of the trace was adjusted on the storage oscilloscope. Using the method outlined in the BA-2 Instruction Manual [7], the chopper was engaged for calibration. The signal was chopped to simulate a known strain. The vertical vernier

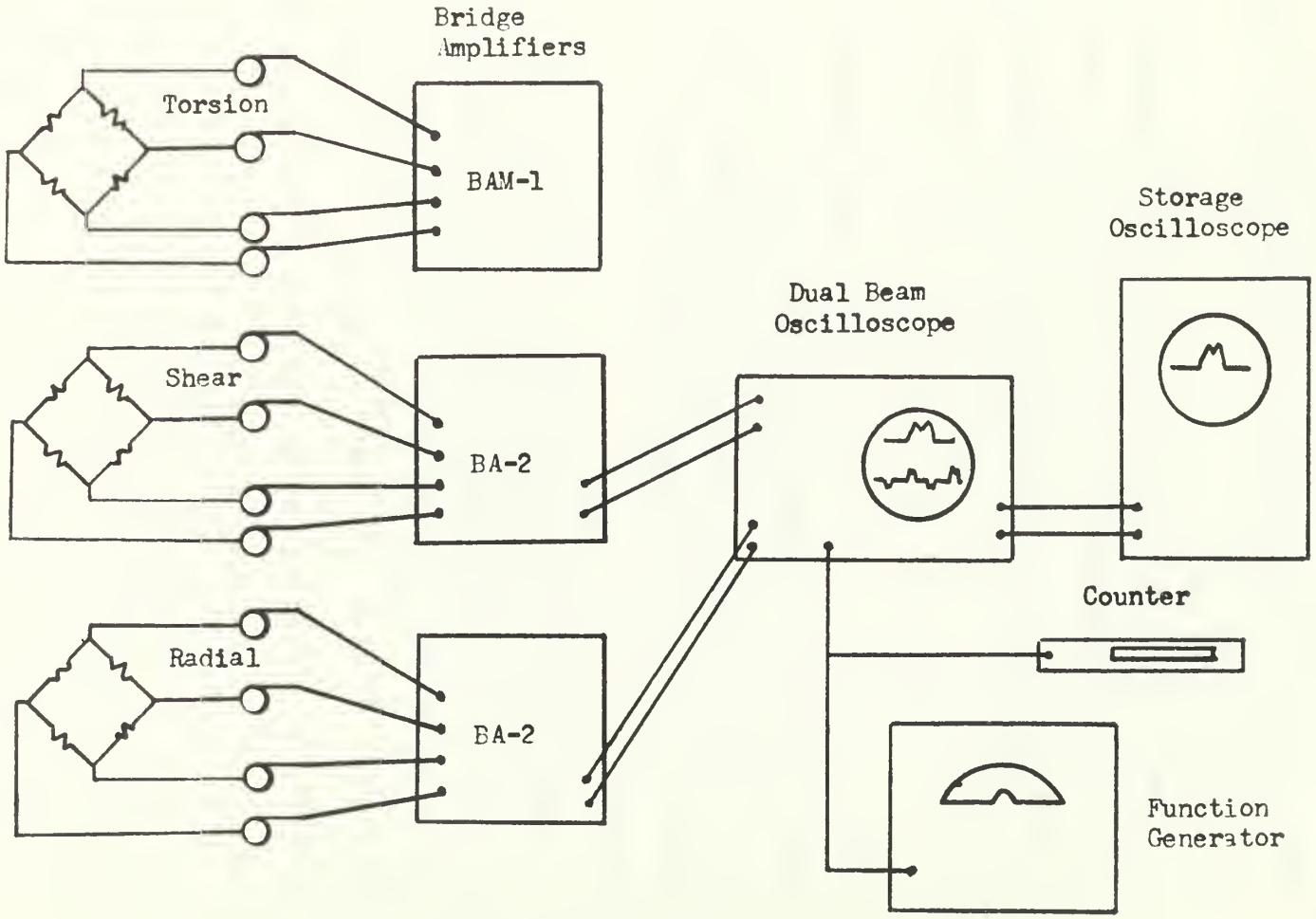

Figure 12. Dynamic Testing Apparatus

on the storage oscilloscope was then adjusted to spread the chopped signal between a convenient number of scope units. The chopper was disengaged and the vertical calibration of the signal was complete. Care was exercised throughout the remainder of the procedure not to touch the vernier and change the calibration.

The storage oscilloscope horizontal time scale, which measured the time in units of milliseconds per horizontal scope division, was used. As a check, the time between repetition of an identical pulse was used to compare the time scale with the shaft speed of rotation.

Before loading the gears, the BAM-1 used to measure the torsional strain was balanced. With the calibration switch on position 1, the calibration switch was depressed and the meter gain adjusted so that the meter read 502 on any convenient scale. This calibrated the BAM-1 to read directly in units of inch pounds. Appendix C contains the calculation of the BAM-1 calibration value.

Upon completion of these adjustments, the gears were loaded. A hand tachometer was used to determine the approximate speed of rotation. The counter was started after the sweep on the dual beam oscilloscope had been stabilized. The trace was stabilized, stored on the screen of the storage oscilloscope, and photographed. The speed of the testing machine was then increased and the process was repeated.

The speed was increased in steps of about 200 RPM up to 1000 RPM. The slowest speed attainable was dependent upon the load but was in the vicinity of 60 RPM.

At speeds over 300 RPM the output from the torsion bridge became erratic. The BAM-1 reading was completely in error. A BLH type "N" indicator was substituted but it was also unreliable above 300 RPM.

When the testing machine was slowed down after completing the high speed runs, the type "N" indicator did settle down and the magnitude of the load could be checked for comparison with the load applied at the beginning of the run. The BAM-1 would not restabilize at or even near the proper values.

The low frequency response of the BA-2 amplifier is poor below 5 Hertz [7]. It can be shown that the speed of 60 RPM is close to this frequency. The values of the lowest speed run, therefore, should be questioned.

6. Analysis.

Figure 13 shows the outputs of the shear bridge and the radial bridge for one complete revolution of the gear. Points A represent the outputs from the calibrated tooth. This pulse will be shown in detail later. Point C indicates the output from the other tooth instrumented with both radial and shear gages. Points B and D represent the outputs from the two compensating gages of the radial bridge.

The signal from the radial bridge was very low in magnitude. High amplification was required to get a discernible trace. Because of the low signal to noise ratio, two of the signals from the radial bridge were obscured by the noise. One of the obscured signals, A, is from the tooth to be used for evaluation of the resultant force. The traces at C and D were good traces but with no previous calibration the data would be meaningless.

With no method available for evaluating the radial force component, the research was continued with the sole purpose of evaluating the transverse component of the dynamic load on the teeth. The signal shown at point A of figure 13 was very good for the shear strain. This trace was photographed following the procedure outlined earlier.

Figures 14 through 19 show the results of increasing speed for a torque of 225 inch pounds. The first two traces are identical except for the horizontal time scale. An attempt was made to search the trace on either side of the pulse in order to find a reason for the negative portion at the end of the pulse. As can be seen from figure 14 with the expanded time scale, no reason is noticeable from the trace.

The first irregularity found when analyzing the traces was that the traces are not as long as they should be. Appendix A lists the pertinent gear data. The tooth should be in contact through an arc of 10.16 degrees

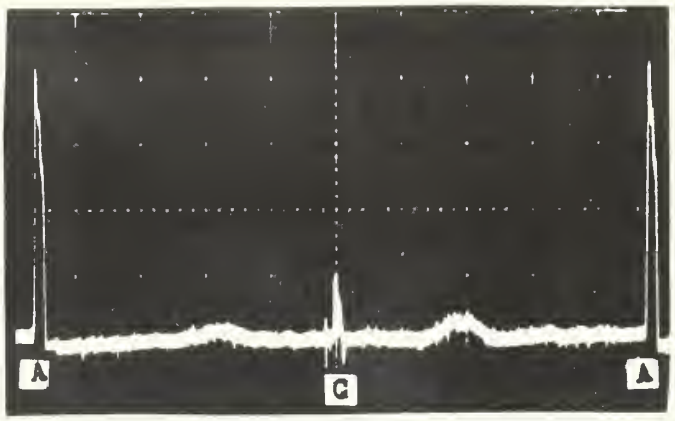

Shear Bridge Trace

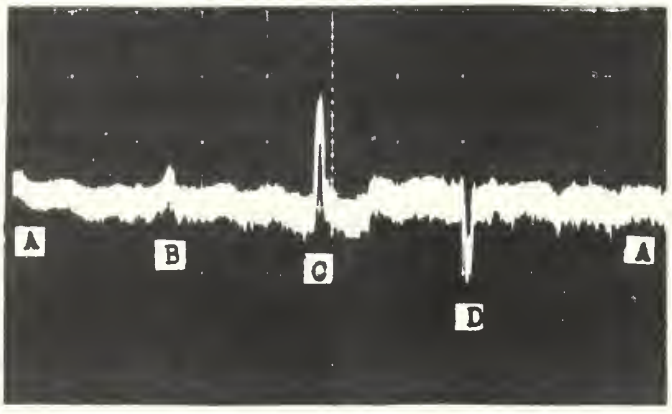

Radial Bridge Trace

Speed 312 RPM
Horizontal Sweep 20 milliseconds/div.
Vertical Sweep 50 microinches/in./div.

Figure 13. Radial and Shear Bridge Traces for One Complete Gear Revolution

of rotation of the gear. In all cases the traces and the time scale indicate contact for only 6 to 7 degrees. In the run made at a heavier load, figures 20 to 25, a dip or hump before or after the trace occasionally can be seen. This irregularity indicates that possibly the arc of contact is greater than that shown by the trace but the force applied to the tooth just after engagement and just before disengagement is very small. None of these trace irregularities could be used reliably to indicate engagement or disengagement of the tooth.

Severe difficulties arose concerning where to enter the calibration curves. If the beginning of the pulse was used as the engagement radius, 2.822 inches, the curves plotted unreliably. It would also be impossible to explain why the teeth disengage very soon after pitch point phase is achieved. Likewise, if the end of the trace is used as the point of disengagement the inverse happened.

After many trial-and-error methods were tried, including the two methods just mentioned, one point was found to plot similarly every time. The second peak on every trace plotted as the point at which the following tooth engages.

Buckingham states that a pressure pulse should result at the time of initial engagement [1]. If this is so, the load on the preceeding tooth should decrease at the same instant. The diving of the calibration curve at low radii could obscure the engagement pulse from the trace. The decrease of load on the preceeding tooth, however, should be distinguishable.

It can be shown that for a very small part of the path of contact, one tooth carries the entire load. This feature is unique with this set of gears. As the instrumented tooth approaches it's pitch point phase, the preceeding tooth disengages. The tooth following the instrumented tooth engages when the gear has rotated 0.5 degrees after passing the pitch point.

The second peak on the trace, where the load begins to decrease, was used as the time of engagement of the following tooth. From this position the pitch point was located and used as a reference for entering the calibration curves to obtain meaningful results.

The relationship between the radius to the point of contact and the angular rotation of the gear is not strictly linear. However, if calculated and plotted, the deviation from linearity is very small. Therefore the assumption of linear relationship between these two parameters was made. The results of the experiment were plotted as tangential force versus radial distance to the point of contact. Time could be used just as easily as radius but the position of the force on the tooth would be somewhat obscured.

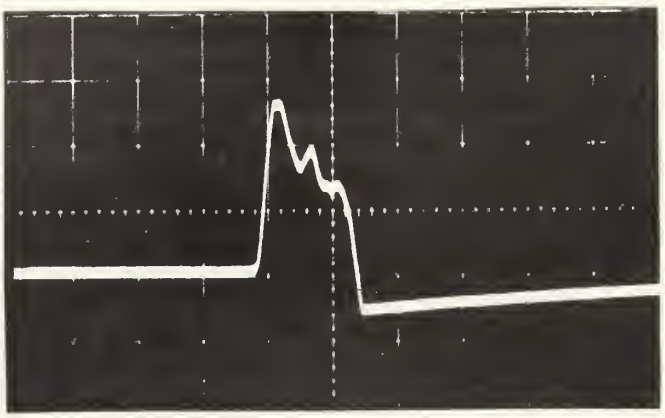

Figure 14
Speed 63.5 RPM
Horizontal Sweep 10 milliseconds/div.
Vertical Sweep 50 microinches/in./div.
Transmitted Load 77.6 pounds

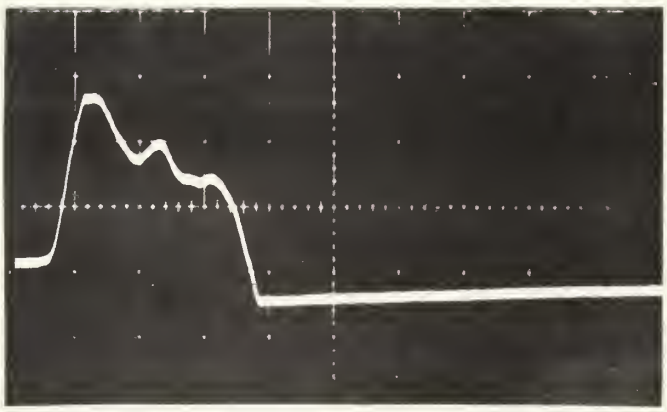

Figure 15
Speed 63.5 RPM
Horizontal Sweep 5 milliseconds/div.
Vertical Sweep 50 microinches/in./div.
Transmitted Load 77.6 pounds

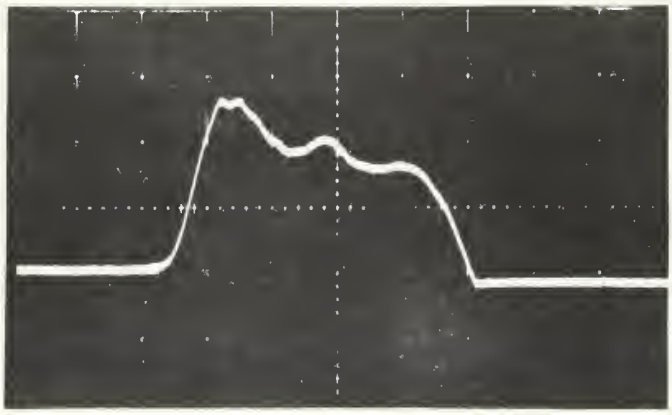

Figure 16
Speed 221 RPM
Horizontal Sweep 1.0 milliseconds/div.
Vertical Sweep 50 microinches/in./div.
Transmitted Load 77.6 pounds

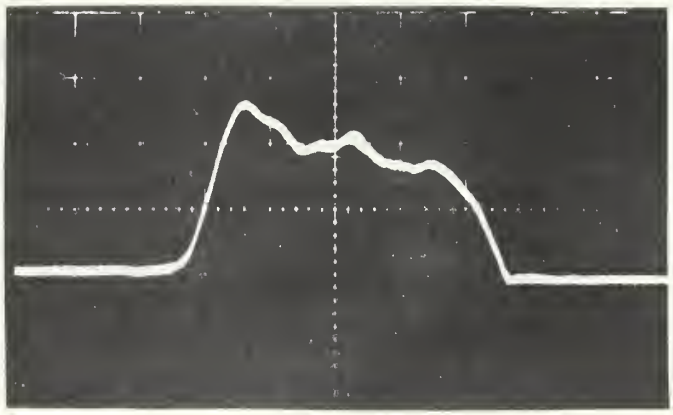

Figure 17
Speed 418 RPM
Horizontal Sweep 0.5 milliseconds/div.
Vertical Sweep 50 microinches/in./div.
Transmitted Load 77.6 pounds

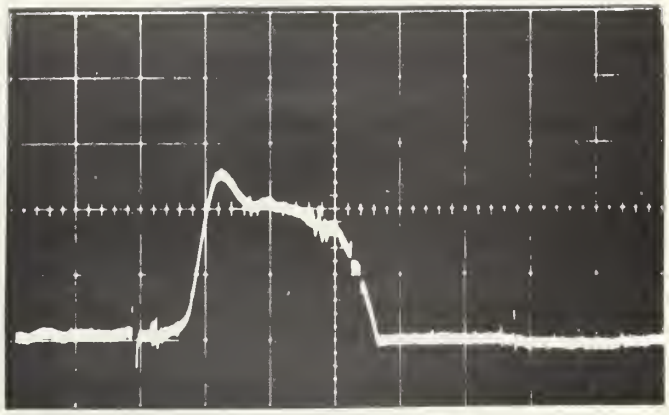

Figure 18
Speed 697 RPM
Horizontal Sweep 0.5 milliseconds/div.
Vertical Sweep 50 microinches/in./div.
Transmitted Load 77.6 pounds

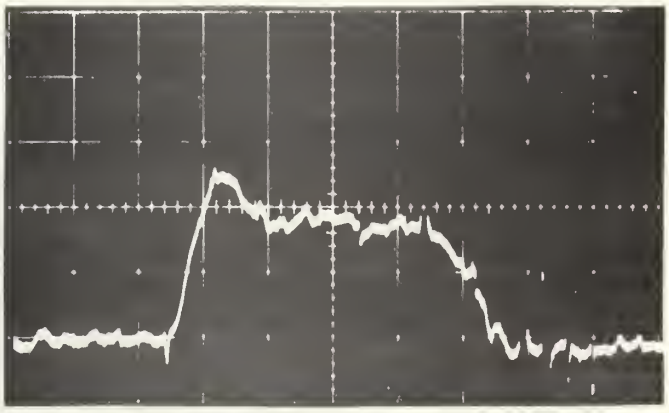

Figure 19
Speed 996 RPM
Horizontal Sweep 0.2 milliseconds/div.
Vertical Sweep 50 microinches/in./div.
Transmitted Load 77.6 pounds

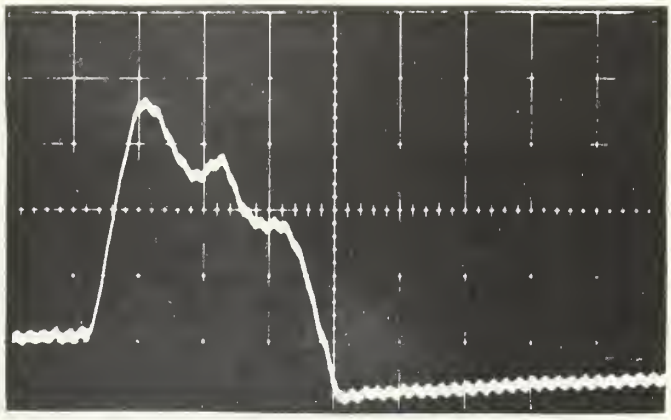

Figure 20
Speed 56 RPM
Horizontal Sweep 5.0 milliseconds/div.
Vertical Sweep 50 microinches/in./div.
Transmitted Load 114 pounds

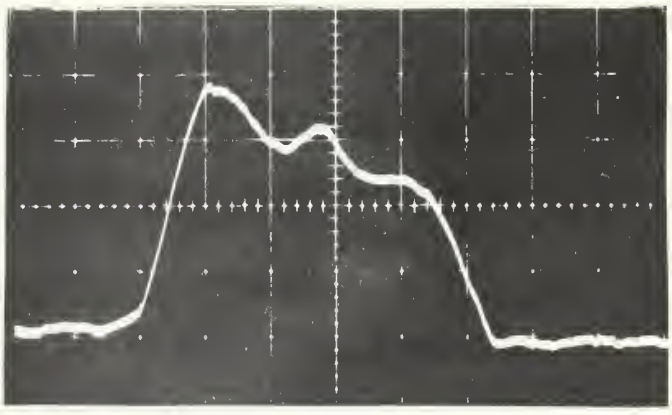

Figure 21
Speed 204 RPM
Horizontal Sweep 1.0 milliseconds/div.
Vertical Sweep 50 microinches/in./div.
Transmitted Load 114 pounds

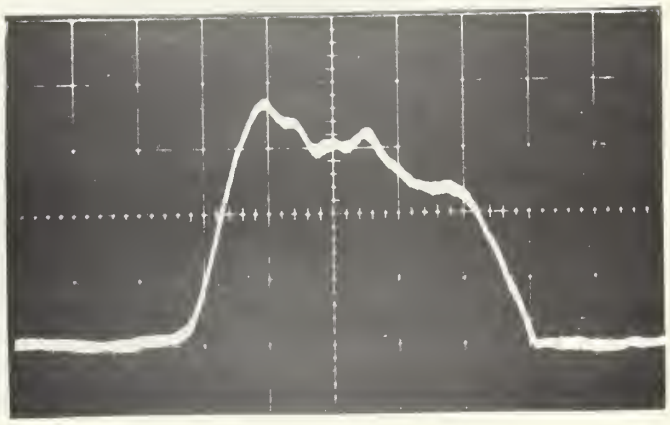

Figure 22
Speed 711 RPM
Horizontal Sweep 0.5 milliseconds/div.
Vertical Sweep 50 microinches/in./div.
Transmitted Load 114 pounds

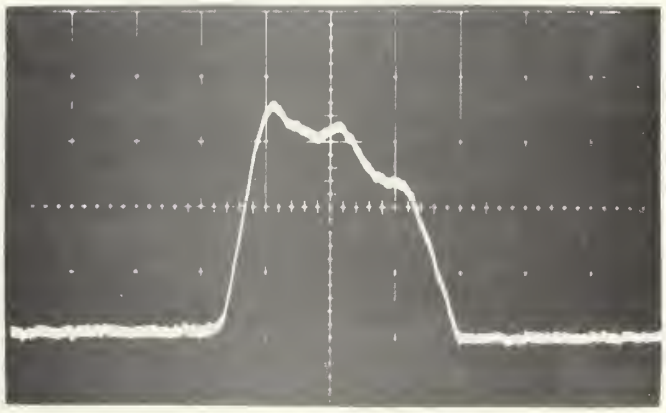

Figure 23
Speed 596 RPM
Horizontal Sweep 0.5 milliseconds/div.
Vertical Sweep 50 microinches/in./div.
Transmitted Load 114 pounds

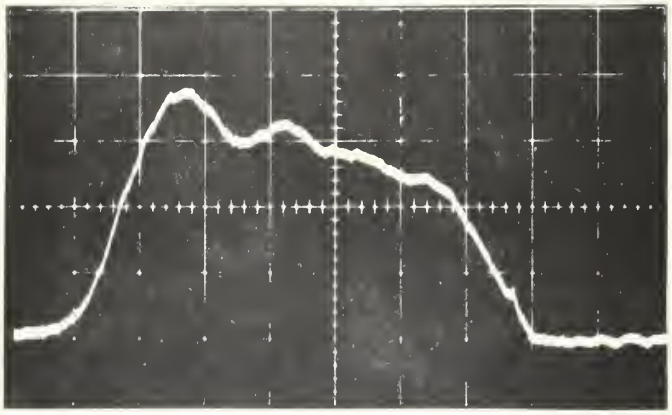

Figure 24
Speed 796 RPM
Horizontal Sweep 0.2 milliseconds/div.
Vertical Sweep 50 microinches/in./div.
Transmitted Load 11¼ pounds

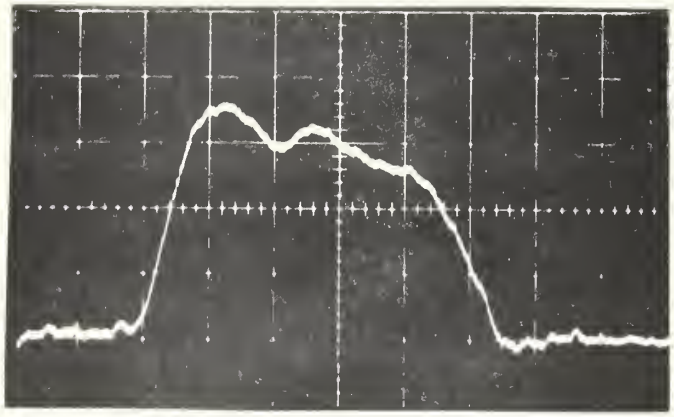

Figure 25
Speed 1000 RPM
Horizontal Sweep 0.2 milliseconds/div.
Vertical Sweep 50 microinches/in./div.
Transmitted Load 11¼ pounds

7. Results

The results of the dynamic tests are as follows:

Transmitted Load Ft,lb	Speed of Rotation, RPM	Dynamic Load, Fd,lb.	Dynamic Load Ratio, Fd/Ft
77.6	63.5	91	1.17
	221	98	1.26
	418	97	1.25
	697	113	1.46
	996	93	1.20
114	56	135	1.18
	204	172	1.51
	411	176	1.54
	596	168	1.47
	796	174	1.53
	1000	178	1.56

Figure 26 shows the comparison between the experimentally obtained dynamic load ratios and the values obtained from the Buckingham equation and the AGMA equation. Disregarding the low speed runs, the ratios are all between 1.20 and 1.60. The experimentally obtained ratios are close to the values obtained from the AGMA equation but are much lower than those obtained from the Buckingham equation. The dynamic load ratio does not increase with speed as much as is indicated by the Buckingham equation but remains essentially the same within the range of the speeds used in this investigation.

The plots of force distribution along the tooth face are shown in figures 27 through 37. Recall that engagement should occur at a radius of 2.822 inches and disengagement should occur at a radius of 2.993 inches.

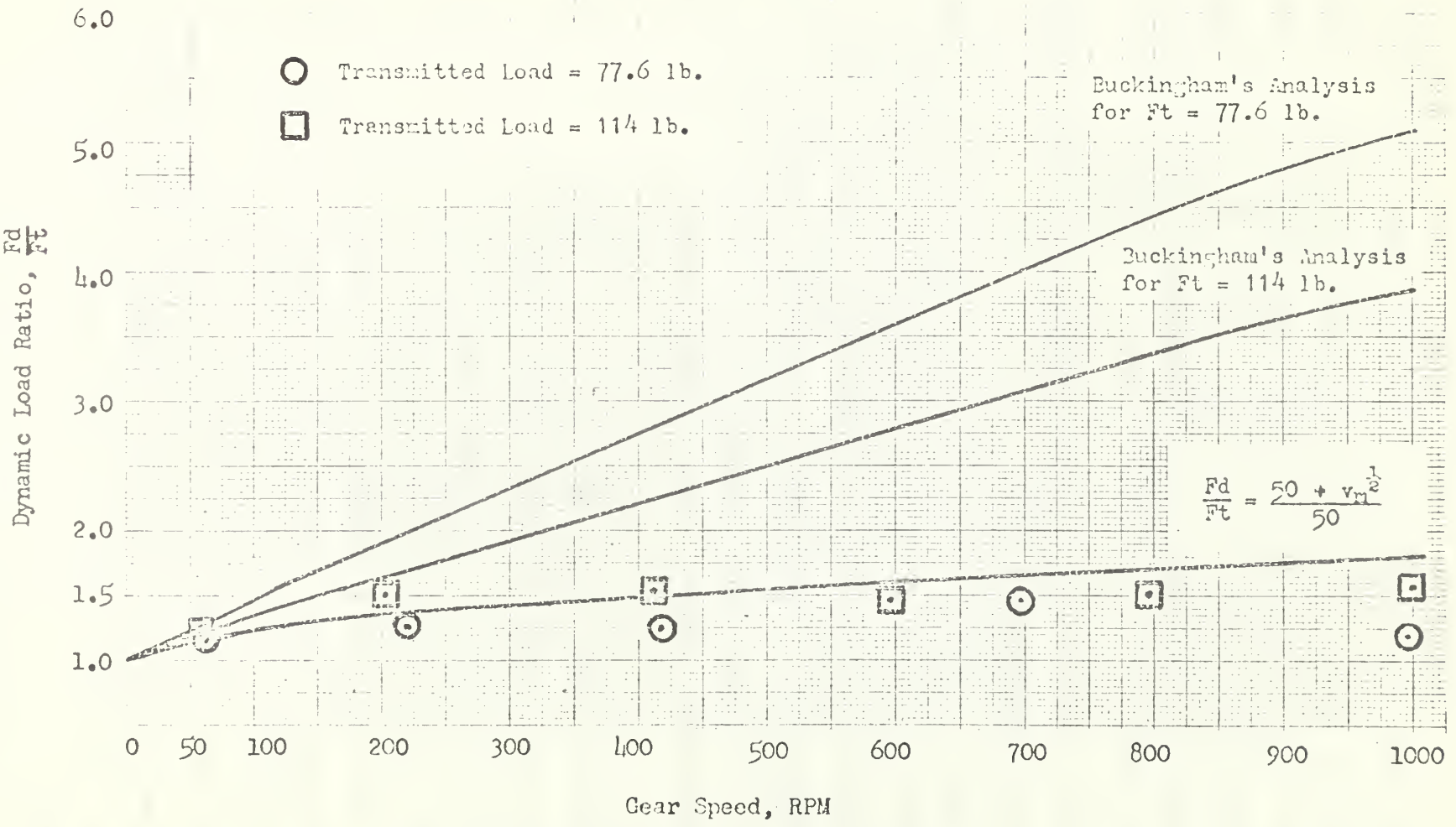

Figure 26. Comparison of Results

It is evident from the loading curves that the maximum load on the tooth occurs slightly after the pitch point phase. It also appears that the tooth carries an increasing portion of the total load as speed increases. This is seen as an increasing height of the plateau to the right of the maximum loading point. For instance, in figure 33 the maximum load peak of 170 pounds is narrow and the subsequent plateau indicates a force of about 140 pounds. As the pitch line speed is increased to 1570 feet per minute in figure 37, the maximum load peak is broader and the plateau is at a force value of 156 pounds.

If the loading curves of three successive teeth are superimposed on one plot the results are as shown in figure 38. The preceeding tooth is moved ahead in time and the following tooth is delayed an amount of time corresponding to one tooth space. This diagram is plotted in horizontal units of radius for easy comparison with figure 33. In figure 38 the slight negative portion of the oscilloscope trace was added. It can be seen that this negative dip occurs right under the first hump of the load distribution curve for the tooth immediately following. There appears to be no reason for this dip other than the possibility of a slight spring back of the tooth as the following tooth picks up a greater portion of the load. This may be the result of the first pressure pulse found by Buckingham.

After one tooth disengages the following tooth passes through the pitch point phase and experiences the second pressure pulse. This pulse produces the maximum load condition. At this time one tooth is transmitting the entire load. This pressure pulse is interrupted by the engagement of the following tooth and a steady load is transmitted for a short period of time. As the tooth reaches the end of the contact path the load falls off rapidly.

The pressure pulse at engagement predicted by Buckingham did not appear

on the oscilloscope traces. The gears in use were reported by the manufacturer to be tip relieved by about 0.0003 inches. This is not enough to account for the trace indicating only 60 to 70 percent of the contact path but it would account for the absence of the initial pressure pulse. This might explain why a slight pressure pulse shows up later and affects the strain gage on the preceeding tooth near its time of disengagement.

The dip at the end of engagement was also found by Pethick [4]. As suggested, it is possible that the stresses transmitted through the gear web do affect the strain gages when the following tooth engages. It is also possible that tooth spring-back produces the negative deflection. It is highly unlikely, however, that the tooth actually experiences a force in the opposite direction. Whatever the cause, the phenomenon has appeared twice with vastly different strain gage orientations.

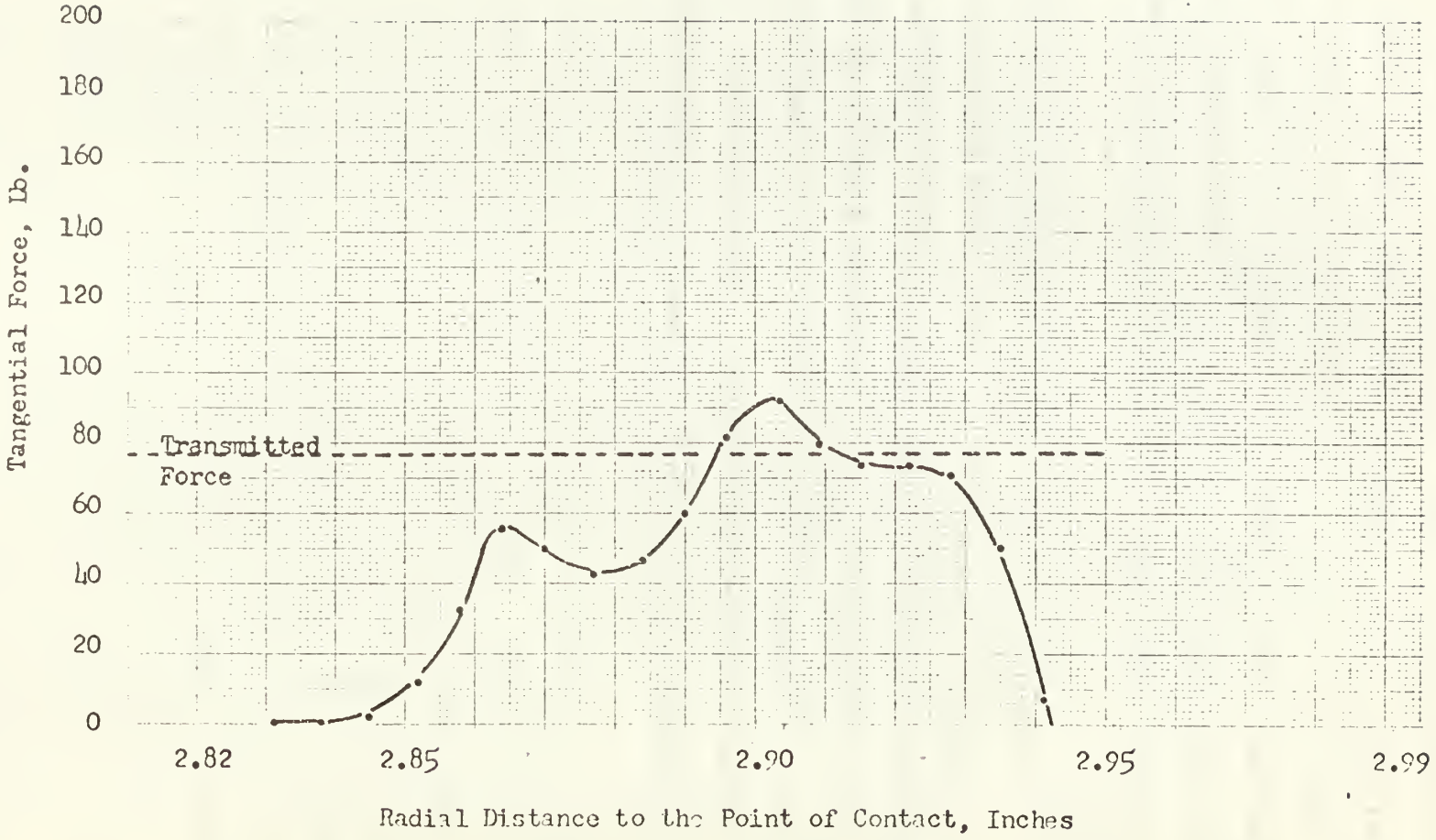

Figure 27. Load Distribution for 63.5 RPM

Figure 28. Load Distribution for 221 RPM

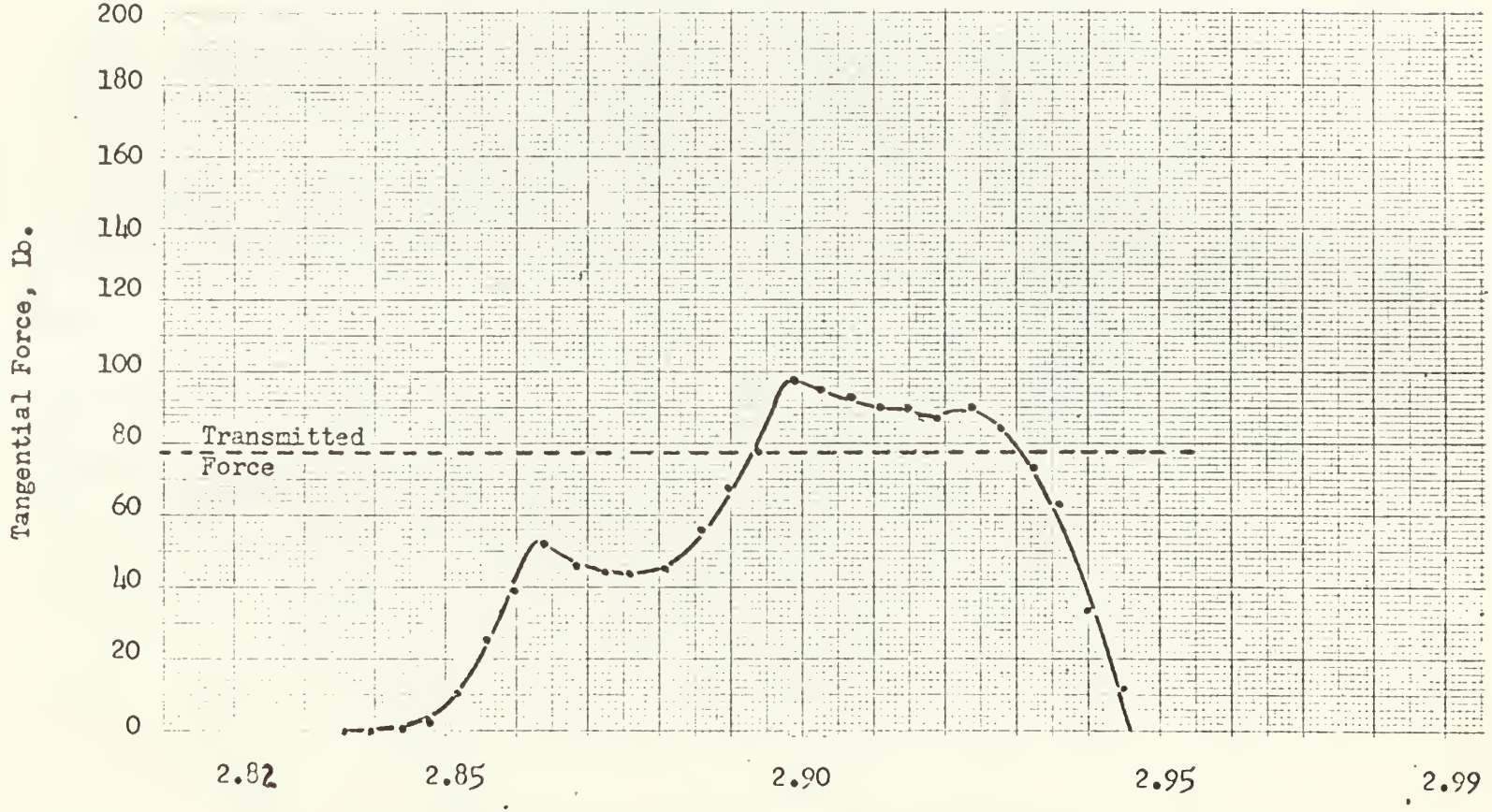

Figure 29. Load Distribution for 418 RPM

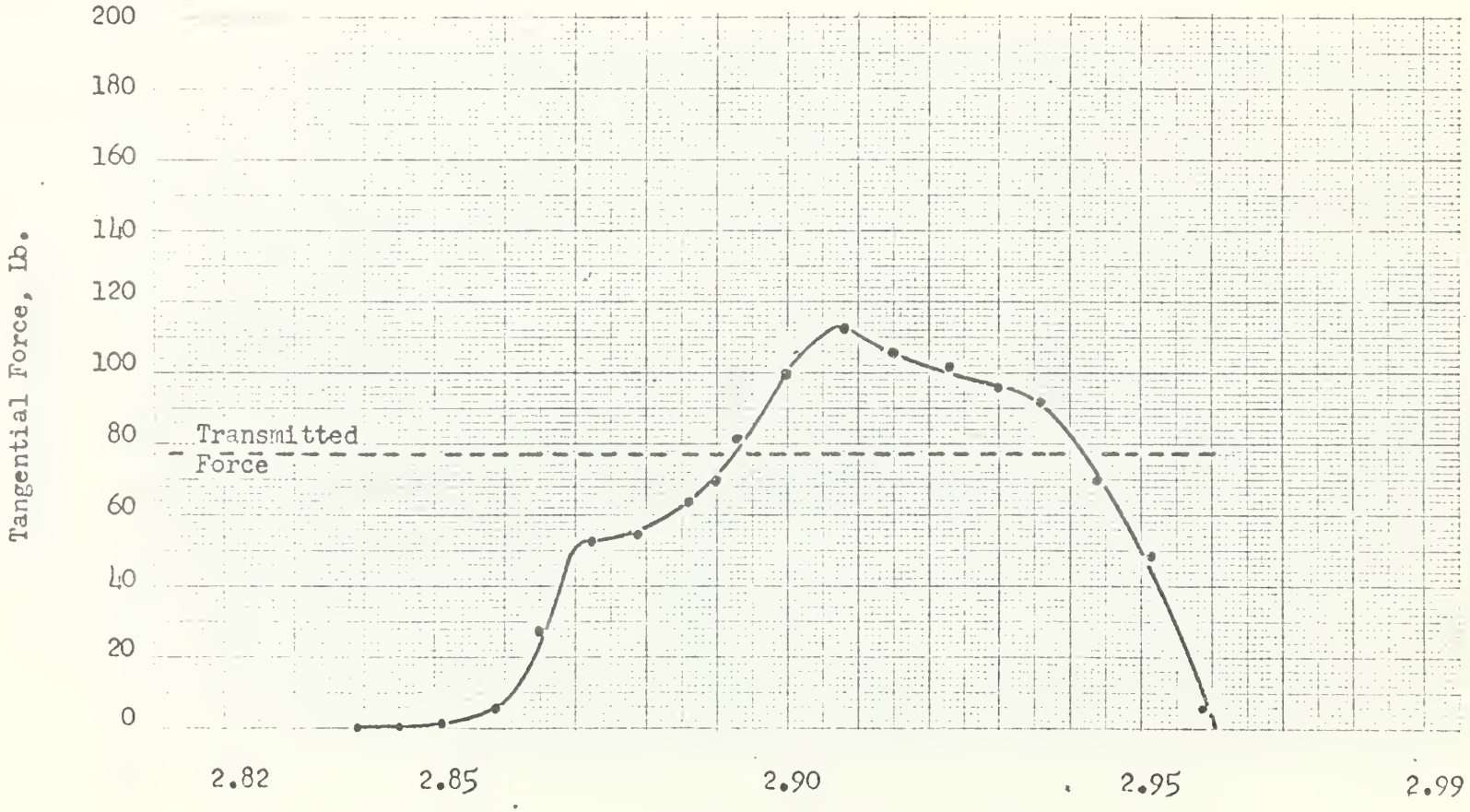

Figure 30. Load Distribution for 697 RPM

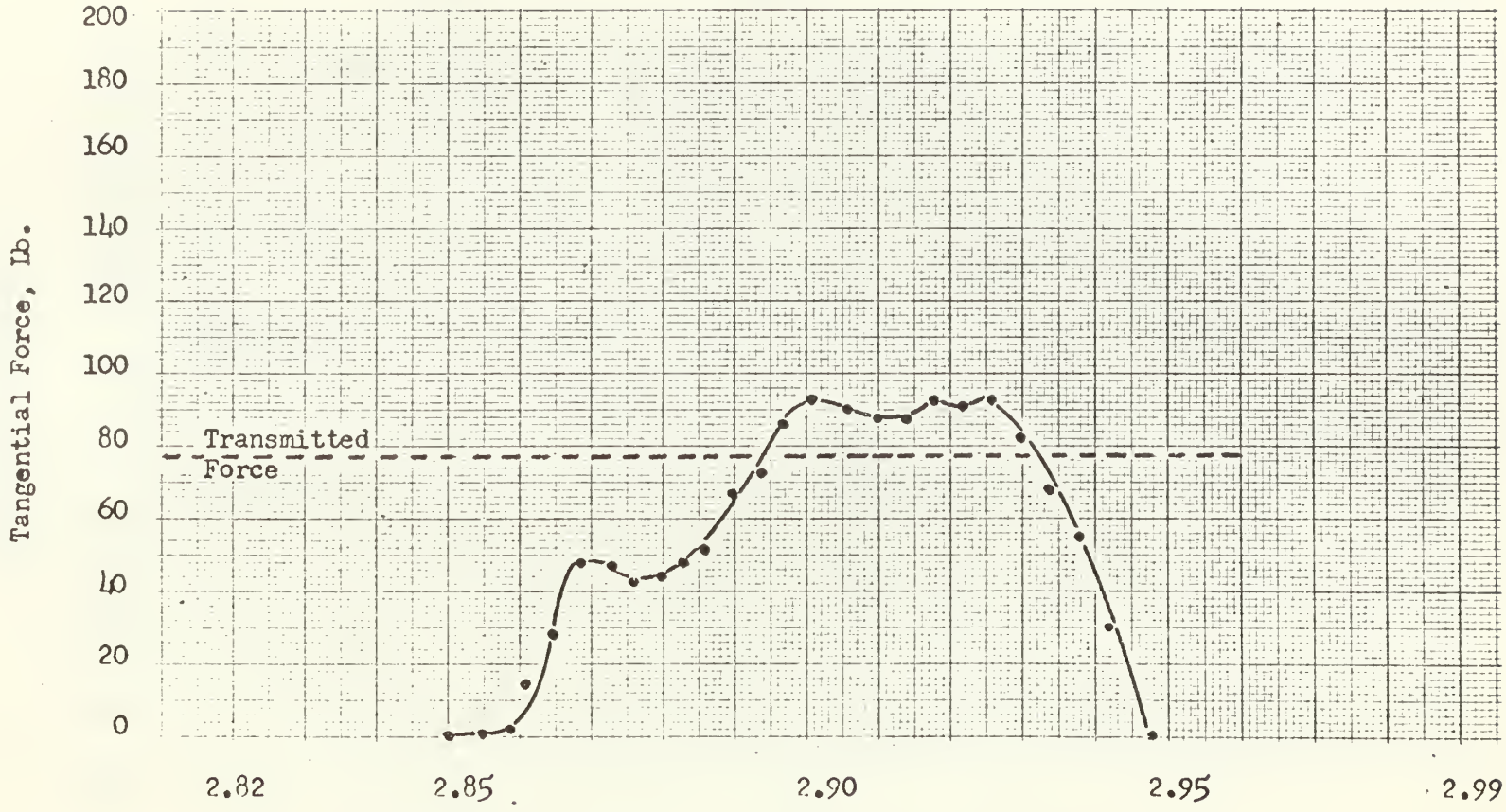

Figure 31. Load Distribution for 996 RPM

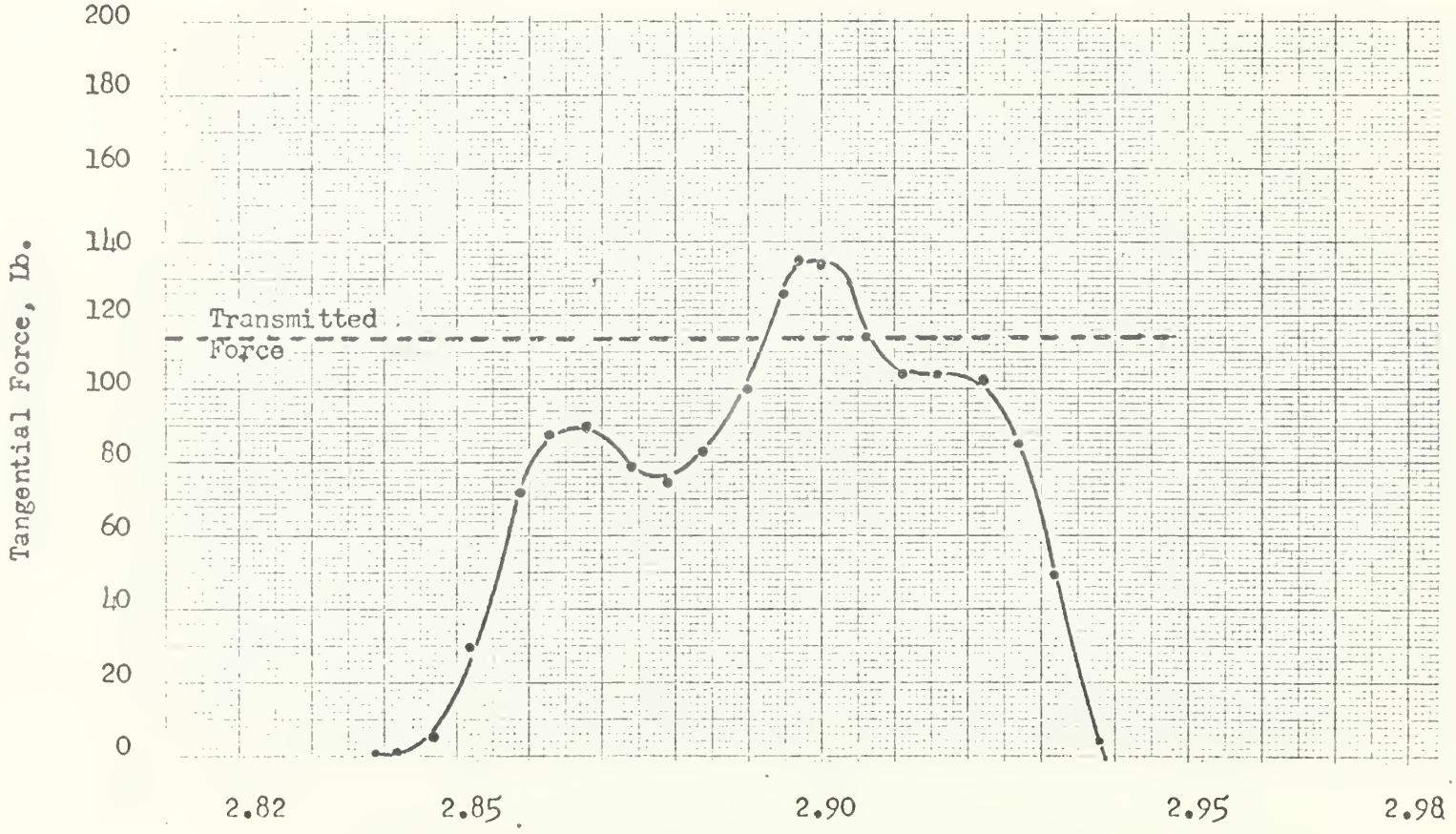

Figure 32. Load Distribution for 56 RPM

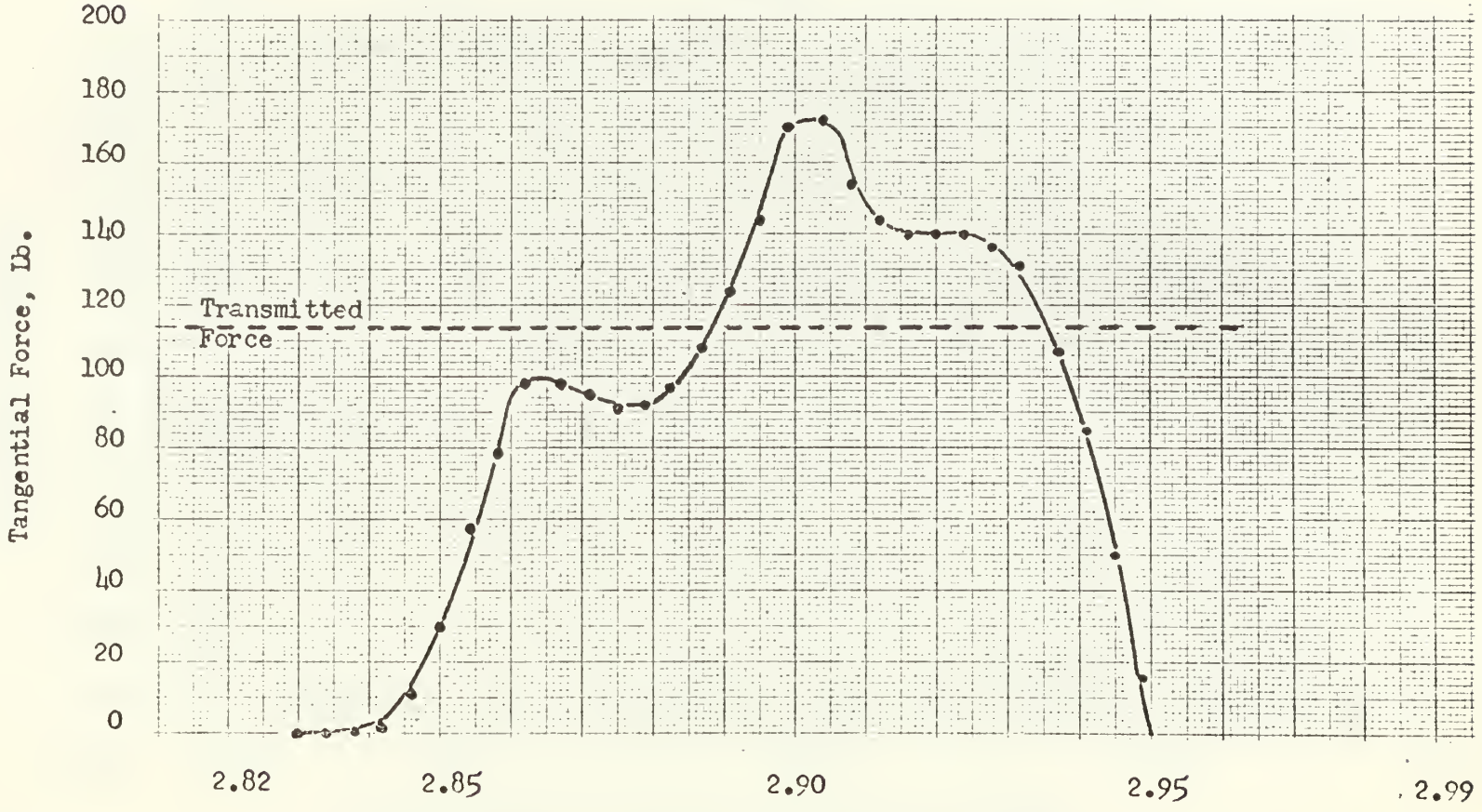

Figure 33. Load Distribution for 204 RPM

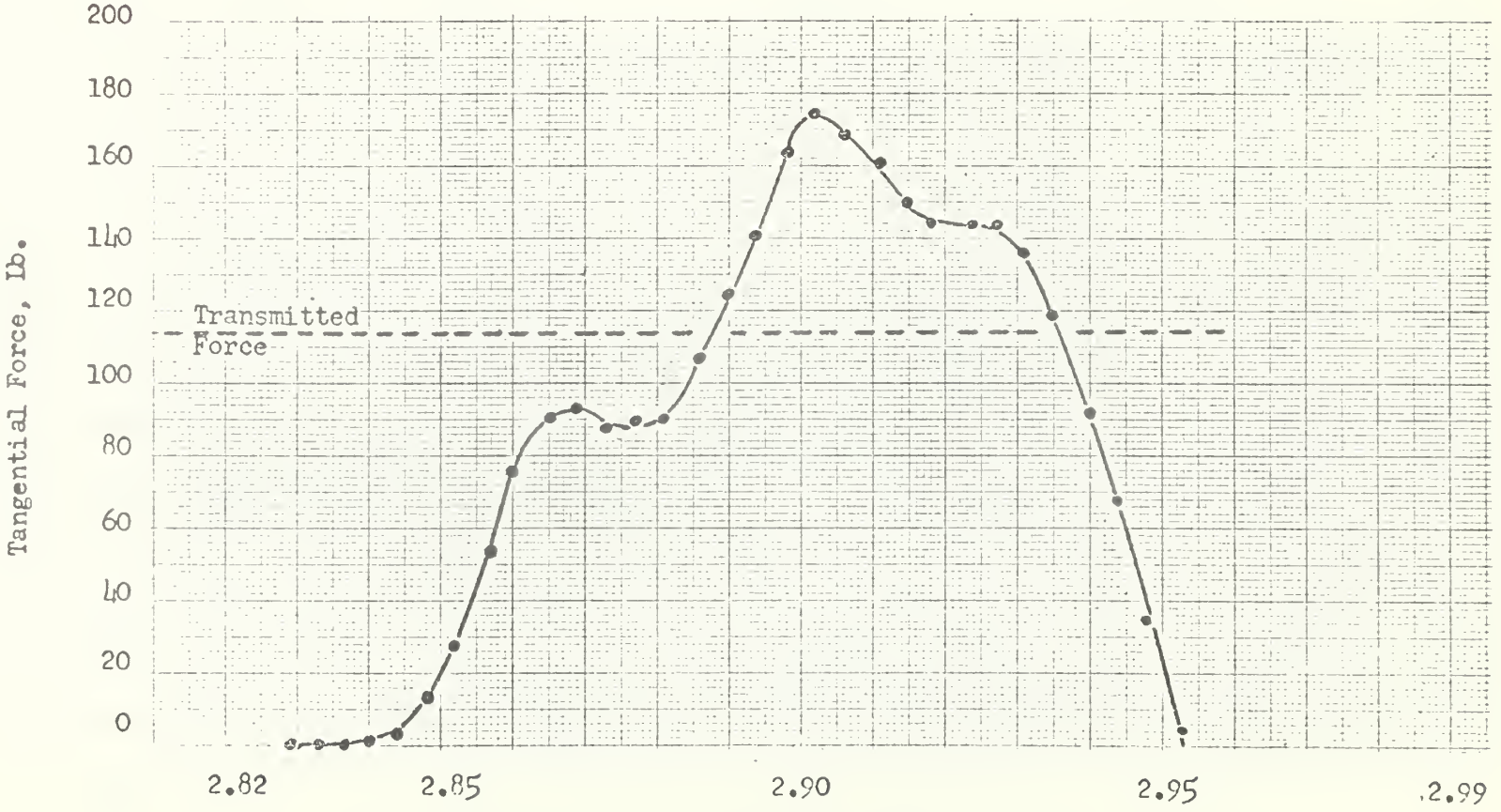

Figure 34. Load Distribution for 411 RPM

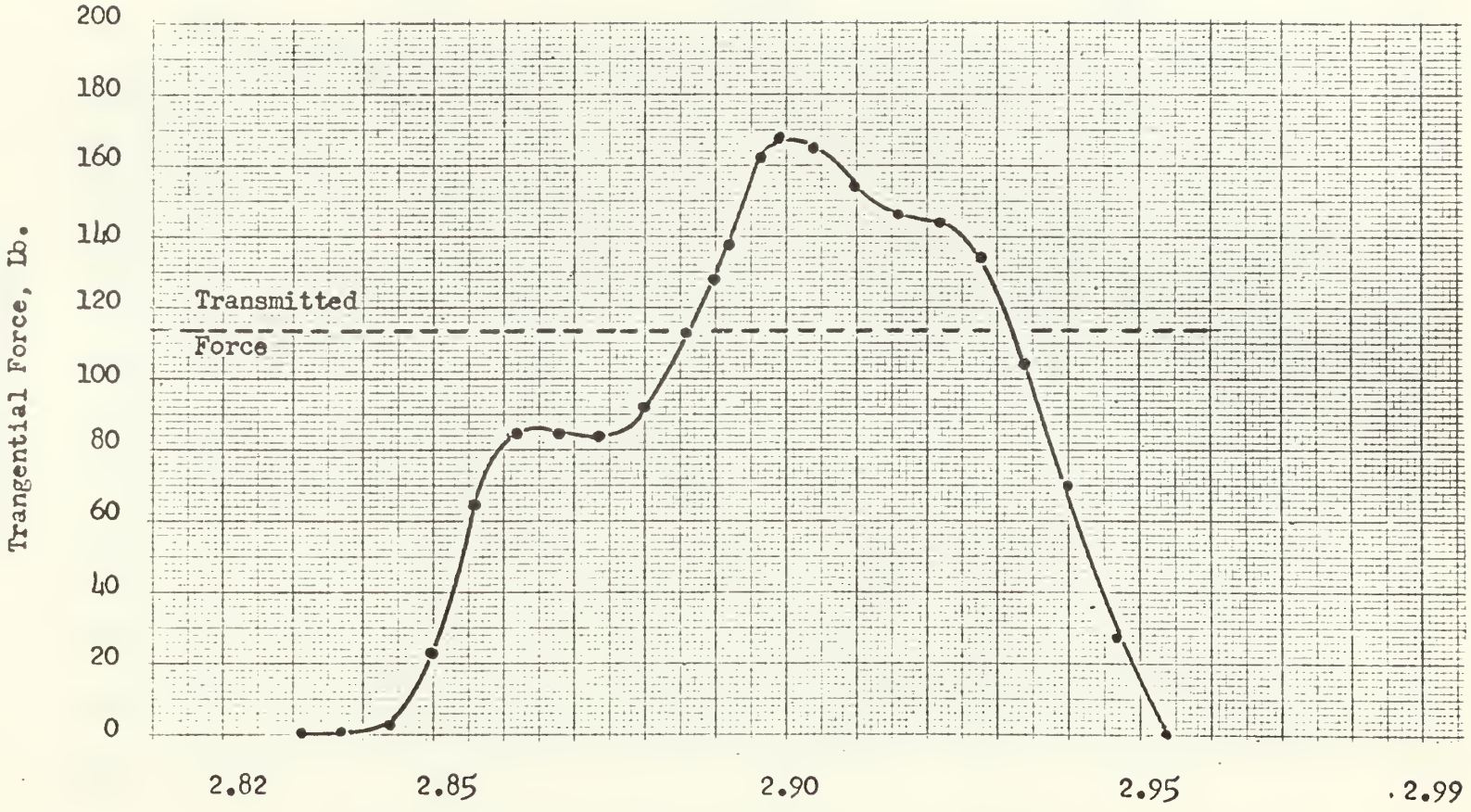

Figure 35. Load Distribution for 596 RPM

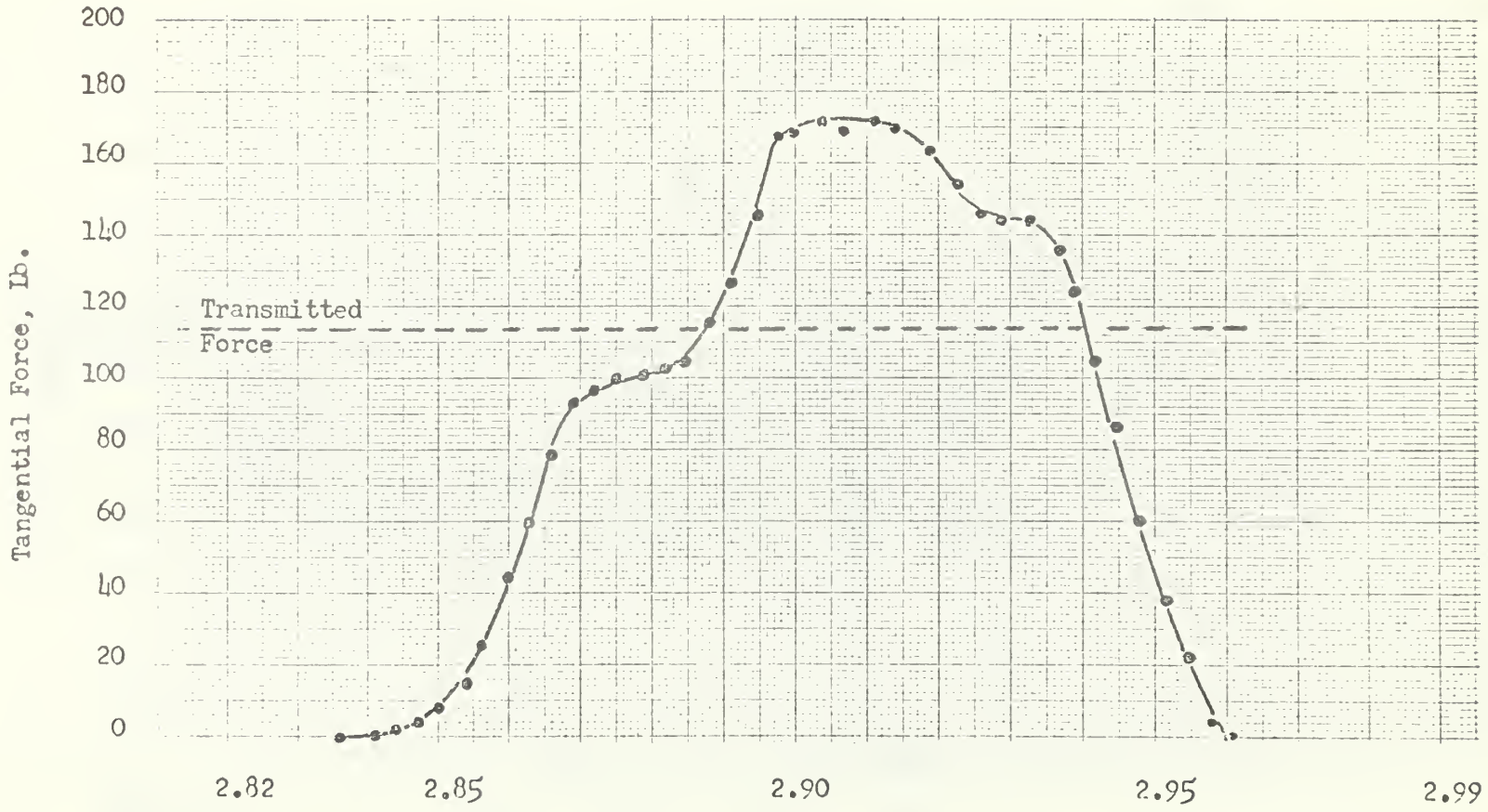

Figure 36. Load Distribution for 796 RPM

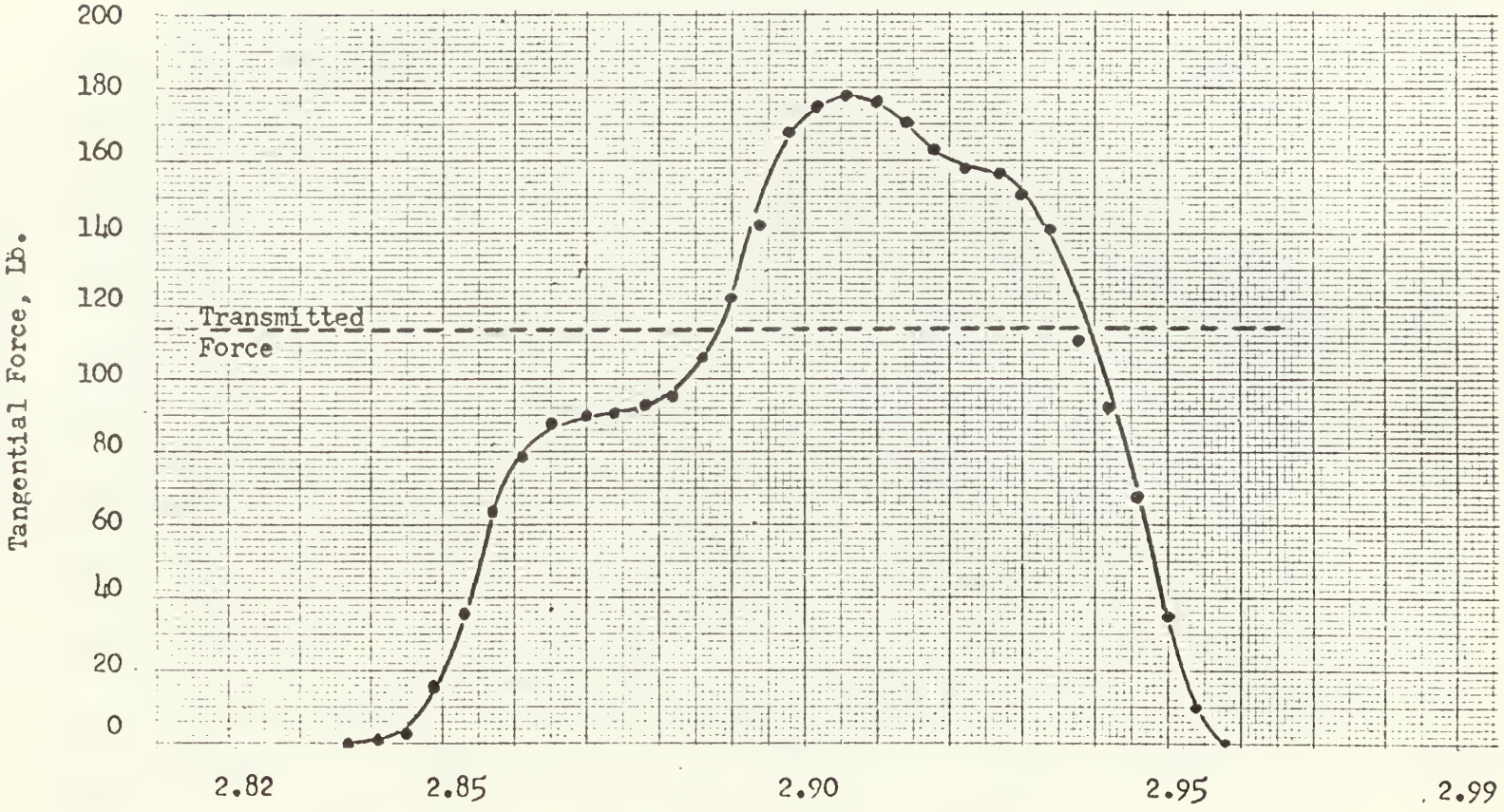

Figure 37. Load Distribution for 1000 RPM

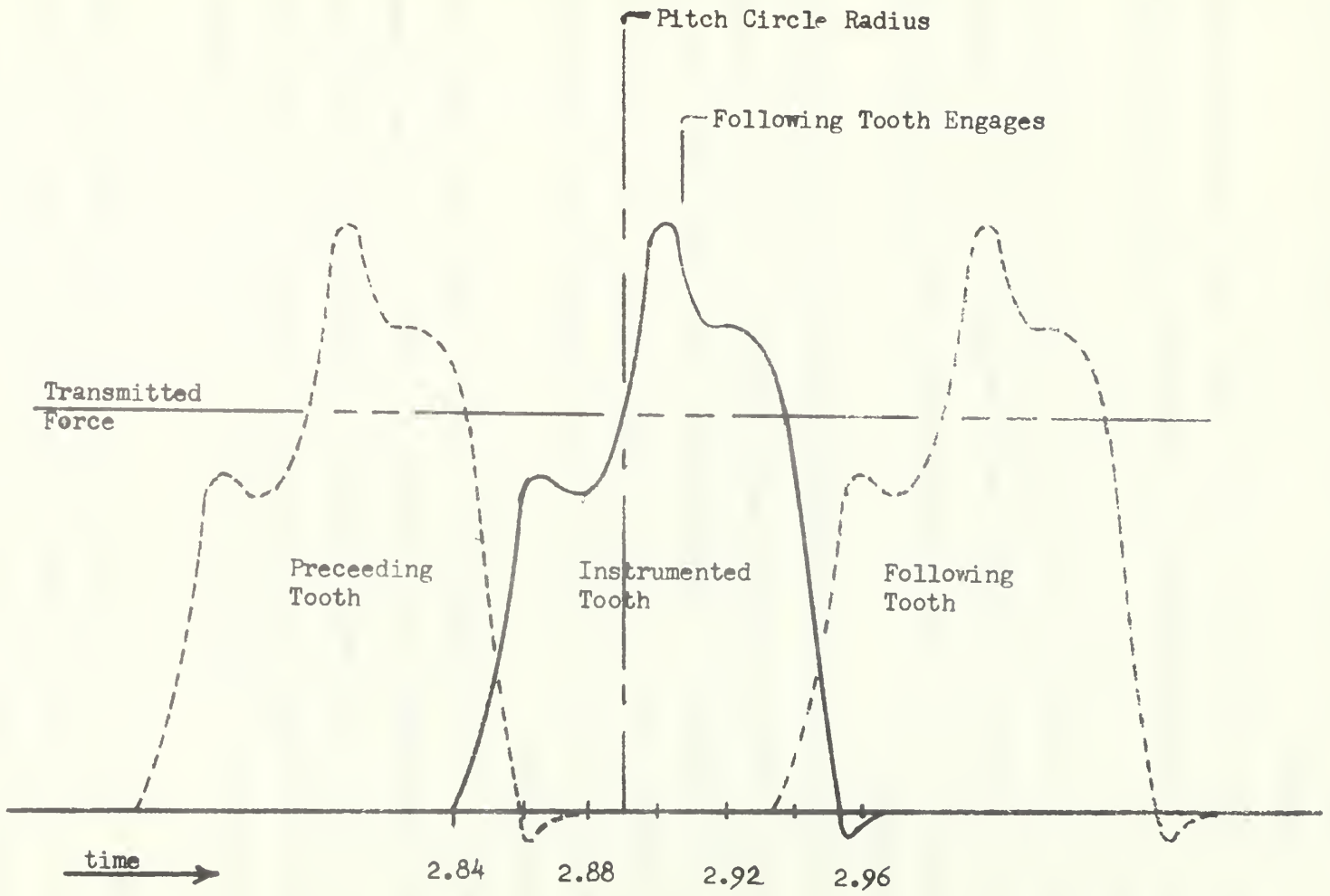

Radial Distance to the Point of Contact, Inches

Figure 38. Superimposed Load Distribution for Three Gear Teeth

8. Conclusions and Recommendations.

Dynamic loads on gear teeth were recorded and measured with the use of strain gages. The tangential force on the tooth was found for all phases of contact.

The dynamic load ratio increased slightly as the pitch line speed increased. As speed increased above 200 RPM the ratio remained between 1.2 and 1.6.

One of the effects of tip relief is to reduce the magnitude of the forces on the tooth at engagement and disengagement. For this particular application, the first pressure pulse on the tooth did not occur until well after engagement.

The maximum load on the tooth was found to occur after the pitch point phase. When the following tooth engaged, the load on the instrumented tooth decreased. By adjusting the contact ratio upward from 1.84 to just slightly under 2.0, the following tooth would pick up part of the load earlier and relieve the load on the instrumented tooth close to the pitch point phase.

Because of the low signal level from the radial force bridge the resultant force acting on the tooth was not found. The method proposed here is believed to be sound. However, the signal magnitude should be increased by increasing the bridge factor or by using strain gages with higher gage factors. Increasing the output by a factor of five would be advised.

Before the gear test machine is used for further experimental work the cause of interference between circuits should be found. Installation of shielded cables where they are not now in use might be justified.

Further work on dynamic loading should be done using different gears. The results for gears having contact ratios above and below that for the gears now in use should be obtained.

BIBLIOGRAPHY

1. Buckingham, Earle Analytical Mechanics of Gears. New York: McGraw-Hill Book Company, Inc., 1949.

2. Faires, Virgil M. Design of Machine Elements. Fourth edition. New York: The Macmillan Company, 1965.

3. Merritt, H. E. Gears. Third edition. London: Sir Isaac Pitman and Sons, Ltd., 1954.

4. Pethick, John A. II, The Construction and Use of a Test Machine to Measure Dynamic Loads on Gear Teeth. Naval Postgraduate School Thesis.

5. Hansen, Harry J. III, The Design of a Four-Square Gear/Lubricant Research Instrument. Naval Postgraduate School Thesis.

6. Timoshenko, S. and D. H. Young, Elements of Strength of Materials. Fourth edition. Princeton, New Jersey: D. Van Nostrand Company, Inc., 1962.

7. Operating Instructions, BA-2 Bridge Amplifier. Ellis Associates. Pelham, N. Y.

8. Instruction Book for BAM-1 Bridge Amplifier and Meter. Ellis Associates. Phelham, N. Y.

APPENDIX A

Gear Data

	Test Drive Gear	Test Gear
Face width, w	0.375 in.	0.375 in.
Pitch diameter, Dp	5.7795 in.	5.7795 in.
Base circle diameter, D_b	5.4309 in.	5.4309 in.
Outside diameter, Do	5.9877 in. 5.9847 in.	5.9877 in. 5.9847 in.
Whole depth, W. D.	0.2083 in.	0.2083 in.
Normal circular tooth thickness, t	0.1440 in. 0.1425 in.	0.1440 in. 0.1425 in.
Backlash with mate	0.003/.005 in.	0.003/.005 in.
Pressure angle, PA	20°	20°
Number of teeth, N	65	65
Pitch error	0.0003 in.	0.0003 in.
Involute profile error	0.0004 in.	0.0004 in.
Lead error	0.0003 in.	0.0003 in.

Center to center distance, C 5.80 in.

Tooth error was measured and found to be 0.0009 inches.

Adjusted pressure angle [3]

$$\phi' = \cos^{-1} \frac{Dp \cos \phi}{C} = \cos^{-1} \frac{(5.779)(0.93969)}{5.80}$$

$$\phi' = 20.55°$$

Base pitch $P_b = \pi \frac{Db}{N} = \pi \frac{(5.4309)}{65}$

$$P_b = 0.262 \text{ in.}$$

Length of action [2]

$$Z = (r_{a2}^2 - r_{b2}^2)^{\frac{1}{2}} + (r_{a1}^2 - r_{b1}^2)^{\frac{1}{2}} - C \sin \phi'$$

Since $r_{a1} = r_{a2}$ and $r_{b1} = r_{b2}$

$$Z = 2(r_a^2 - r_b^2)^{\frac{1}{2}} - C \sin \phi'$$

$$= (D_o^2 - D_b^2)^{\frac{1}{2}} - C \sin \phi'$$

$$= 2.5174 - 2.0359$$

$$Z = 0.4815 \text{ in.}$$

Angle of action

$$\psi_{action} = \psi_{approach} + \psi_{recess} = 2\,\psi_{approach}$$

$$= (2)\,\frac{Z}{D_b} \text{ radian} = (2)\,\frac{(180)}{\pi}\,\frac{(0.4815)}{5.4309}$$

$$\psi_{action} = 10.16°$$

Contact ratio

$$Mc = \frac{Z}{P_b} = \frac{0.4815}{0.262}$$

$$Mc = 1.84$$

Angular tooth spacing $= \frac{360}{65} = 5.538°$

APPENDIX B

Strain Gage Characteristics

The strain gages were manufactured by Baldwin-Lima-Hamilton Co., Waltham, Mass.

Single-element radial strain gages:

Type FAE - 03N - 12S6

Gage factor = 1.94 $\pm$ 2%

Resistance = 120.0 $\pm$ 0.2 ohms

k = 0.8

Two-element shear strain rosettes:

Type FAED - 06 - 12S6

Gage factor = 1.98 $\pm$ 2%

Resistance = 120.0 $\pm$ 0.2 ohms

k = + 1.5

Cement

EPY - 400

Cured at 250° F for 6 hours.

APPENDIX C

BAM-1 Calibration

The four gages on the shaft are oriented 45 degrees above and below the shaft axis and measure plain strain in the principal directions.

For calculating the BAM-1 calibration setting, the following symbols will be used:

- E Modulus of elasticity, $lb/in.^2$
- ϵ_τ Shear strain, in./in.
- τ Shear stress, $lb/in.^2$
- σ stress, $lb/in.^2$
- μ Poisson's ratio
- G Shear modulus, 12,000,000 $lb/in.^2$
- J Polar moment of inertia of the shaft, $in.^4$
- Di Inside diameter of the hollow shaft, 0.50 in.
- Do Outer diameter of the hollow shaft, 2.00 in.
- θ Angle of twist per unit length of the shaft, radians
- Mt Torsional moment, in.-lb

From Hooke's Law $E\epsilon_\tau = \sigma_1 - \mu(\sigma_2 + \sigma_3)$.

For pure shear we have $\tau = \sigma_1 = -\sigma_2$, $\sigma_3 = 0$. Therefore $E\epsilon_\tau = \tau(1+\mu)$

Since $G = \frac{E}{2(1+\mu)}$, we have $\tau = 2G\epsilon_\tau$

For a circular shaft [6] $\tau = \frac{Do}{2} G\theta$ and $\theta = \frac{Mt}{GJ}$. Therefore

$$\tau = 2G\epsilon_\tau = \left(\frac{Do}{2}\right)\left(G\right)\left(\frac{Mt}{GJ}\right) \quad \text{and} \quad Mt = \left(\frac{4GJ}{Do}\right)\epsilon_\tau$$

For a hollow shaft the polar moment of inertia is given by [6]

$$J = \frac{\pi}{32} (Do^4 - Di^4) = 1.565 \text{ in.}^4$$

From the BAM-1 Instruction Manual [8]

$$\epsilon_\gamma = \frac{\text{gage resistance}}{\text{gage factor}} \times \frac{\text{calibration setting}}{\text{number of working arms}} \text{, micro-inches per inch}$$

$$= \frac{120}{2.06} \times \frac{\text{calibration setting}}{4}$$

For a calibration setting of 1,

$$\epsilon_\gamma = 14.56 \text{ microinches/inch}$$

The calibrating value is

$$Mt = \frac{4(12{,}000{,}000)(1.565)}{2.00} (14.56) = 546 \text{ in.lb}$$

The value that should be used is Mt = 502 in.lb, after correcting for the torsion bridge calibration.

INITIAL DISTRIBUTION LIST

		No. Copies
1.	Defense Documentation Center Cameron Station Alexandria, Virginia 22314	20
2.	Library Naval Postgraduate School Monterey, Calif.	2
3.	Professor E. K. Gatcombe Department of Mechanical Engineering Naval Postgraduate School Monterey, Calif.	2
4.	Department of Mechanical Engineering Naval Postgraduate School Monterey, Calif.	2
5.	Naval Ship Systems Command (Code 2052) Navy Department Washington, D. C. 20360	1
6.	LT Paul J. Umberger, USN Philadelphia Naval Shipyard Philadelphia Pennsylvania 19112	2
7.	Rev. G. J. Umberger 28 West Washington St., Fleetwood, Pennsylvania 19522	1

DOCUMENT CONTROL DATA - R & D

(Security classification of title, body of abstract and indexing annotation must be entered when the overall report is classified)

1. ORIGINATING ACTIVITY *(Corporate author)*
Naval Postgraduate School
Monterey, California 93940

2a. REPORT SECURITY CLASSIFICATION
Unclassified

2b. GROUP

3. REPORT TITLE
A Study of Dynamic Loads on Straight Spur Gear Teeth

4. DESCRIPTIVE NOTES *(Type of report and inclusive dates)*
None

5. AUTHOR(S) *(First name, middle initial, last name)*
Umberger, Paul Jay

6. REPORT DATE	7a. TOTAL NO. OF PAGES	7b. NO. OF REFS
June 1968	74	8

8a. CONTRACT OR GRANT NO.	9a. ORIGINATOR'S REPORT NUMBER(S)
b. PROJECT NO. N/A	N/A
c.	9b. OTHER REPORT NO(S) *(Any other numbers that may be assigned this report)*
d.	

10. DISTRIBUTION STATEMENT
This document is subject to special export controls and each transmittal to foreign governments or foreign nationals may be made only with prior approval of the Naval Postgraduate School.

11. SUPPLEMENTARY NOTES	12. SPONSORING MILITARY ACTIVITY
N/A	Naval Postgraduate School Monterey, California 93940

13. ABSTRACT

The dynamic loads acting on gear teeth are very complex. To better understand dynamic loads, this research was carried out with the objectives of measuring experimentally dyamic loads and the frictional forces between gear teeth in mesh. By using strain gages mounted on the sides of the teeth, the transverse component of the dynamic load was measured and is shown for all phases of contact. Using the transverse component at the pitch radius, the dynamic load ratios were computed and found to be substantially lower than predicted by the Buckingham equation. However, sufficient information for evaluating the frictional force was not obtained and further research will be required to evaluate the radial component of the dynamic load.

14. KEY WORDS	LINK A		LINK B		LINK C	
	ROLE	WT	ROLE	WT	ROLE	WT
Gear						
Gear Load						
Dynamic Load						